



Manuel Eibinger, BSc

# **Insights into the role of single enzymes during the enzymatic cellulose degradation**

Atomic force microscopy based investigation of a novel multiphasic substrate

Masterarbeit

zur Erlangung des akademischen Grades eines  
Diplomingenieurs

erreicht an der

Technischen Universität Graz

betreut durch:

Univ.-Prof. DI Dr. Bernd Nidetzky  
Institut für Biotechnologie und Bioprozesstechnik  
Technische Universität Graz

## EIDESSTÄTTLICHE ERKLÄRUNG

Ich erkläre an Eides statt, dass ich die vorliegende Arbeit selbstständig verfasst, andere als die angegebenen Quellen/Hilfsmittel nicht benutzt, und die den benutzten Quellen wörtlich und inhaltlich entnommene Stellen als solche kenntlich gemacht habe.

Graz, am .....

.....

(Unterschrift)

### STATUTORY DECLARATION

I declare that I have authored this thesis independently, that I have not used other than the declared sources / resources, and that I have explicitly marked all material which has been quoted either literally or by content from the used sources.

.....  
date

.....  
(signature)

## Zusammenfassung

Zellulose ist ein Biopolymer, welches vor allem in pflanzlichen Zellwänden in Form von Fibrillen vorkommt. Diese Fibrillen sind in eine amorphe Matrix, aus anderen Biopolymeren (z.B. Lignin), eingebettet. Starke molekulare Interaktionen zwischen diesen Biopolymeren führen zu einem unlöslichen und sehr komplexen Substrat, dessen Nutzung limitiert ist. Daher haben spezielle Mikroorganismen, wie etwa holzverwertende Pilze, Systeme entwickelt, um Zellulose in Glukose zu konvertieren. In Zeiten der globalen Energiekrise und dem wachsenden Verlangen nach einem nicht auf Erdöl basierenden Energieträger, sind jene Systeme vielversprechende Kandidaten unseren Bedarf nach einer erneuerbaren Energiequelle zu befriedigen.

Im Zuge dieser Studie fokussierten wir uns auf den industriellen Produzenten von Zellulasen (*Trichoderma sp.*), welcher in den letzten zwei Dekaden Gegenstand zahlreicher Untersuchungen war. Dabei benutzten wir eine neuartige Substrat, das uns erlaubte die Aktivität von Zellulasen auf einer gemischt kristallin-amorphen nanoflachen Oberfläche, zu studieren. Diese speziellen Oberflächeneigenschaften ermöglichten uns den Einsatz von Rasterkraftmikroskopie, begleitet von umfangreichen Hydrolysen und Proteinadsorptionsstudien.

Diese Kombination von verschiedenen Methoden erlaubte uns neue Einblicke über Substratspezifitäten, aber auch über die Aufgaben während des Zelluloseabbaus, der untersuchten Enzyme zu erhalten.

## Abstract

In plant cell walls, cellulose is organized into fibrils, which are embedded in an amorphous matrix of other structural biopolymers (e.g. lignin). Strong interactions between fibres and those structural features lead to a complex and insoluble substrate, thus limiting its microbial utilization. Microorganisms such as wood-rotting fungi developed cellulase systems which are capable of degrading cellulose into glucose. In times of global energy shortage and increasing demand for non-oil-based fuel, those systems are promising candidates to satisfy our urgent need for a renewable energy source (e.g. cellulosic ethanol).

In our work we focus on the fungal cellulase system of *Trichoderma* sp. which has been a subject of extensive studies over the last decades using a combination of various biochemical assays and different types of imaging techniques. We used a new substrate preparation which provides us with the unique opportunity to study enzymatic activities on a mixed mainly amorphous and crystalline substrate with a nano-flat surface. In our work we performed an atomic force microscopy based investigation with accompanying hydrolysis and protein adsorption studies. This combination allowed us to achieve new insights about the substrate preferences of the probed cellulases and a first allocation of individual activities during cellulose degradation towards single cellulolytic enzymes on our novel substrate.

## Acknowledgements

This thesis would not have been possible without the support of many people. First and foremost I want to thank my thesis advisors, Univ.-Prof. Dipl.-Ing. Dr. Bernd Nidetzky and Dipl.-Ing. Dr. Patricia Bubner, for their guidance, support, patience, and helpful suggestions during the work on this thesis and my time at the institute.

Secondly I would also like to acknowledge all the members of the Institute of Biotechnology and Biochemical Engineering at the Graz University of Technology for their support.

I also would like to thank Dipl.-Ing. Dr. Harald Plank and Thomas Ganner, BSc for their good cooperation and providing me deeper insights into atomic force microscopy based imaging techniques.

Further I would like to thank the Institute of Molecular Biotechnology (Graz University of Technology) which generously provided the cellulolytic enzyme CBH II.

Finally, I would like to express my gratitude to my friends and family. Thank you for always believing in me and offering your support. My special appreciation goes to my parents, Martina Ceru-Eibinger and Peter Ceru, for all their support over the time.

# 1 Table of contents

2	Draft for a manuscript.....	9
2.1	Introduction.....	10
2.2	Material and Methods.....	12
2.2.1	Materials.....	12
2.2.2	Enzyme preparation .....	12
2.2.3	Preparation of the model cellulose substrate.....	13
2.2.4	Enzymatic hydrolysis .....	13
2.2.5	Rate calculation .....	15
2.3	Results and Discussion .....	15
2.3.1	The complete cellulase system of <i>T. reesei</i> SVG17 .....	15
2.3.2	CBH I .....	17
2.3.3	CBH II .....	20
2.3.4	EG I.....	21
2.4	Conclusions.....	22
2.5	References.....	33
3	Appendix A –Real time observation of enzymatic cellulose degradation.....	36
3.1	Introduction.....	36
3.2	Material and Methods.....	37
3.2.1	Materials.....	37
3.2.2	Enzyme preparation .....	37
3.2.3	Atomic force microscope (AFM).....	38
3.2.4	AFM image analyses.....	38
3.2.5	Preparation of the model substrate.....	39
3.3	Results and Conclusion.....	40
3.3.1	SVG17 .....	40
3.3.2	CBH I .....	47
3.3.3	CBH II .....	49
3.3.4	EG I.....	53
4	Appendix B – Purification of CBH I .....	57

---

4.1	Introduction.....	57
4.2	Material and Methods.....	57
4.2.1	Materials.....	58
4.2.2	Enzyme preparation .....	58
4.2.3	Purification of CBH I .....	58
4.2.4	Protein concentration .....	59
4.2.5	Enzymatic activity assays.....	59
4.3	Results .....	60
4.4	Results and Discussion .....	62
4.5	Conclusions.....	63
5	References.....	64
6	Supporting Information.....	67
6.1	Protein sequence of CBH II expressed in <i>Pichia pastoris</i> .....	67
7	Abbreviations .....	68

## 2 Draft for a manuscript

### ***Trichoderma sp.* single cellulase enzymes probed on a novel multiphasic substrate**

Manuel Eibinger<sup>1</sup>, Patricia Bubner<sup>1</sup>, Bernd Nidetzky<sup>1</sup>

<sup>1</sup>*Institute of Biotechnology and Biochemical Engineering, Graz University of Technology, Petersgasse 12, A-8010 Graz, Austria; E-mail: manuel.eibinger@student.tugraz.at*

#### **Abstract**

Cellulose is an abundant natural biopolymer of  $\beta$ -1,4 linked glucose which is exclusively produced biosynthetically: either by photosynthesis as in higher plants and algae or non-photosynthetically as in certain microorganisms. Most abundant in plant cell walls, cellulose is organized in fibrils embedded in an amorphous matrix of other structural biopolymers (e.g. lignin). Strong interactions caused by those structural features leading to a very complex and insoluble substrate where cellulose utilization is limited. Fungal systems which are able to convert cellulose into glucose have been targeted by researches using various methods over the last decades. In our work we focused on a typical fungal system produced by *Trichoderma sp.* which can be considered as the most potential producer of cellulases nowadays. Moreover, we used a novel nano-flat substrate, which has been subject of recent research, providing us with the unique opportunity to study cellulolytic behaviour on mixed crystalline amorphous substrates. Further this substrate allowed us to investigate the influence of structural features on individual probed enzymes. As reference substrate, we used microcrystalline cellulose (Avicel), which has been widely employed as a substrate standard. This combination allowed

us to achieve new insights about the substrate preferences of CBH II and a first allocation of individual activities during cellulose degradation towards single enzymes on our novel substrate.

## 2.1 Introduction

In times of global energy shortage and increasing demand for non-oil-based fuel, cellulose seems to be an ideal candidate to satisfy our urgent need for a new renewable bioenergy source [1]. Naturally abundant in plant cell walls, cellulose is organized into fibrils, which are intertwined in an amorphous matrix of other structural biopolymers like lignin or hemicellulose [2]. Strong interactions between those structures lead to a complex and insoluble substrate, thus limiting its utilization by different chemical, biological and even combined technical approaches [3]. Accordingly, microorganisms such as wood-rotting fungi developed sophisticated cellulase systems which are capable of degrading cellulose into glucose. These systems comprise three types of hydrolytic enzymes working in a cooperative manner (“synergistically”). However, there are still limitations to their industrial exploitation, mainly enzyme costs and insufficient conversion rates [4].

The enzymatic degradation of cellulose has been targeted by various research approaches: from the early hydrolysis studies [5] to elucidation of structure and function of the involved enzymes [6]. Recently, atomic force microscopy (AFM) has started to play a more important role [7] in revealing details of the degradation process. Studies of cellulose and cellulases on a mesoscopic up to a molecular level provide us with a deeper insight of what single cellulolytic enzymes are actually doing on substrates [8]. Previous AFM studies used mainly crystalline cellulose providing novel insights into the mode of action of CBH I. Out of this

arose the demand for new substrates combining the presence of ordered and unordered regions.

Therefore we used a novel cellulose preparation which had been designed as a model substrate for AFM studies [9]. This substrate provides us with the unique opportunity of studying the behavior of cellulolytic enzymes on mixed amorphous-crystalline (MAC) cellulose. Moreover this substrate allows us to study the influence of structural features on a cellulose surface. For instance we were able to show the influence of amorphous matrix parts covering fibrils. Moreover, our MAC substrate allows us to study enzymatic behavior on a defined nano-flat surface.

Previous studies of a fungal cellulose degradation system based on this substrate recommended a new kind of stepwise cellulose degradation. Out of this arises a demand of closing the lack of knowledge about basic kinetic parameters and protein binding profiles of single enzymes on the MAC substrate. These data might allow us to allocate different task during enzymatic hydrolysis to single enzymes.

Thus, we investigated how a complete cellulase system of *Trichoderma sp.* (*T. reesei* SVG 17 and *T. longibrachiatum*) and its isolated major activities (CBH I, CBH II, EG I) [2] degrade this mixed amorphous-crystalline substrate. As reference substrate, we used microcrystalline cellulose (Avicel), which has been widely employed as a substrate standard.

This combination of substrates allowed us to achieve new insights about substrate preferences of single enzyme compounds and a first allocation of the individual tasks of the probed enzymes on this novel substrate.

## 2.2 Material and Methods

### 2.2.1 Materials

Citric acid, sodium citrate and sodium hydroxide were purchased from Carl Roth, Karlsruhe, Germany. Avicel PH-101 and 1-butyl-3-methylimidazolium chloride (BMIMCl) were obtained from Sigma-Aldrich, Vienna, Austria. Sodium potassium tartrate, phenol and 3,5-dinitrosalicylic acid (DNS) was purchased from Merck, Vienna, Austria.

### 2.2.2 Enzyme preparation

CBH I and EG I (isolated from *T. longibrachiatum*) were obtained from Megazyme International, Dublin, Ireland and stored until further use by 4 °C. The lyophilisate of CBH II (protein sequence [Supporting Information 6.1]) isolated from *T. reesei* and expressed in *P. pastoris* was a gift of the Institute of Molecular Biotechnology (Graz University of Technology) and stored until further use by – 20 °C. Before use the enzymes were subjected to buffer exchange using a NAP-25 columns purchased from GE Healthcare, Vienna, Austria. Buffer exchange was performed according to the manufactures protocol.

The complete cellulase system from *Trichoderma reesei* SVG17 was produced as described by Esterbauer *et al.* [10] and supplemented with 0.05 % sodium azide for storage at 4 °C. Protein concentration was determined to be 0.48 g/l using a “Bovine Serum Albumin” (BSA) calibrated Bradford Assay [11]. Activity was determined, as recommended by IUPAC, using the well established “filter paper units” (FPU) assay [10]. According to this assay, our cellulase system had 1.0 FPU/ml.

### 2.2.3 Preparation of the model cellulose substrate

The substrate was prepared according to Prasad *et al* [9] by dissolving 0.13 g Avicel PH-101 (i.e. 13 % w/w) in 1.0 g BMIMCl by heating at 100 °C for 24 hours with stirring in an air condition controlled room at 23 °C. Secondly, we cut this so called primary gel into squares with a side length of approximately 5 mm and an average thickness of 250 µm. Afterwards the solvent and loosely bound water molecules were removed using a fractionated ethanol extraction protocol (stepwise increase from 30 % to absolute ethanol). Following these secondary gels were air-dried and analyzed using STA and XRD analysis to confirm purity and present cellulose allomorphs as described previously by Bubner *et al* [12].

### 2.2.4 Enzymatic hydrolysis

All hydrolysis experiments were performed discontinuously at 50 °C in 1.5 ml Eppendorf tubes (Eppendorf AG; Hamburg, Germany) at pH 5.0 in 350 µL 50 mM sodium citrate buffer. A fixed substrate concentration of 0.72 g/l was used for both substrates. Sampling was performed at for each enzyme individual defined time points but mainly after 0, 1, 2, 3, 5, 10, 24 and 72 hours.

The reaction was stopped by centrifugation (1 minute at 10000 rpm) and subsequent withdrawal of the supernatant. 150 µl of the supernatant was removed for a triplet determination of the protein binding using a BSA calibrated Bradford assay (200 µl Bradford reagent was added to 50 µl sample and incubated at room temperature for 15 minutes) on a Fluostar Omega platereader (BMG Labtech, Ortenberg, Germany) at a wavelength of 595 nm. The remaining 200 µl was boiled for seven minutes at 95 °C and centrifuged for 1 minute at 10000 rpm. 120 µl of the supernatant was removed and used for determining the degree of conversion using a 96-well-plate adapted glucose calibrated DNS assay [13] and further HPLC analysis for sugar composition.

As shown in Table 1, different enzyme loadings were chosen to achieve a better time resolution of differences between the single cellulolytic activities in terms of chemical analysis and atomic-force-microscopy-based investigations.

#### **2.2.4.1 DNS assay**

The DNS assay was performed to detect reducing sugars released during hydrolysis. A sample aliquot of 20  $\mu\text{l}$  was added to 40  $\mu\text{l}$  50 mM sodium citrate buffer at pH 5.0 in a 96-well plate. Secondly 120  $\mu\text{l}$  DNS reagent was added and the plate was sealed using an aluminium sealing tape obtained from Sigma-Aldrich, Vienna, Austria. Afterwards the plate was incubated at 95  $^{\circ}\text{C}$  for 5 minutes using an iCycler (Biorad, Berkeley, USA). Following colour development, a 36  $\mu\text{l}$  aliquot of each sample was transferred to the wells of a 96-well plate containing 160  $\mu\text{L}$  of distilled water and the absorbance at 540 nm was measured in Fluostar Omega platereader (BMG Labtech, Ortenberg, Germany). A calibration equation was generated by using glucose concentrations varying from 0.1 up to 5 g/l.

#### **2.2.4.2 Sugar composition analysis**

The sugar composition was analysed using a Dionex LC25 Chromatography Oven, an EG40 Eluent Generator, an ED50 Electrochemical Detector, a GS50 Gradient Pump and an AS50 Auto Sampler with a CarboPac PA10 column obtained from Thermo Fisher Scientific Inc., Olten, Switzerland. The samples were diluted with Milli-Q water (Millipore Corporation, Billerica, USA) and separated by an isocratic flow of a 0.148 M sodium hydroxide solution. Retention time was approximately 8.5 minutes for glucose and 26.2 min for cellobiose.

### 2.2.5 Rate calculation

We defined the point of rate retardation to determine a point from then on the hydrolysis could be considered as stopped. This point is reached from then on the hydrolysis rate drops below 15 % of the initial rate during the first hour. The rates are achieved using a simple differential equation. Two initial rate values were calculated for EG I due to the presence of a lag phase (Figure 2b and 5). We calculated one value over the first hour containing the lag phase, the second value was calculated based on the data points at one and three hours to exclude the lag phase (Table 1).

$$r_c = \frac{\frac{(Conv_x - Conv_{x-1})}{(t_x - t_{x-1})}}{P_x}$$

**Equation 1.** Equation used to calculate the rate ( $r_c$ ) and the point of rate retardation. Conversion (Conv), protein adsorbed to the substrate (P), time (t) and indices (x) indicating the time point.

## 2.3 Results and Discussion

### 2.3.1 The complete cellulase system of *T. reesei* SVG17

We applied the complete fungal cellulase system of *T. reesei* to observe effects of the predicted synergism toward both substrates. The time course of enzymatic Avicel hydrolysis is shown in Figure 1a, additionally the time course over the first five hours is emphasized in Figure 1b to provide a higher resolution of the initial phase of the hydrolysis. It can be clearly seen that the degradation process performed by the whole cellulase system is more efficient in terms of reaching a higher conversion than performed by single enzymes. Figure 1b also

shows that the whole system reaches a higher initial rate even with a loading 10 up to 100 fold lower than the single enzyme loadings.

The time course of the MAC substrate is shown in Figure 2a and the first five hours of the conversion are highlighted in Figure 2b. As already seen in the Figures 1a and 2a shows the cellulase system the highest initial rate and is able to reach the highest conversion in comparison to the single enzyme compounds (Table 1). The point of rate retardation was reached on both substrates after 24 hours of incubation.

As shown in Figure 4, we observed a step like conversion function during the first five hours of the MAC substrate hydrolysis. Moreover we observed a step like protein binding over the same time span. Interestingly, we detect a temporary stop of the increase of bound protein at the same time where we detect a plateau in the conversion curve. A possible interpretation is that enzymes modify the complex substrate in terms of generating new surface, followed by an increase of bound protein resulting in an increase of the hydrolysis rate. This is in a good agreement with previous studies performed on the MAC substrate [12].

The difference in the degradation efficiency of the complete system as compared to its single components separately is clearly observable on both substrates. Even with loadings up to 100 fold higher (CBH II on MAC, Figure 2) the degradation efficiency of the combined enzymes cannot be achieved (Table 1). This phenomenon has long been known and is called synergism – the cooperative action of cellulases to achieve the degradation of their insoluble substrate [2].

Interestingly - although not surprising - the conversion reaches a higher level on the multiphasic substrate. This might be explained by the higher conversions of the single enzymes compounds (e.g. EG I). As shown in Table 1 EG I reached after 24 hours a 23 fold higher conversion on the MAC substrate than on the microcrystalline Avicel. This substrate

degradation preference might occur due to the higher abundance of amorphous parts. This is supported by the comparison of the crystalline indices (CI) of the used substrates. Avicel is known to have a CI varying between approximately 70 up to 90 %. Our MAC substrate has a CI of about 20 % [14]. However this is a qualitative information and could not be directly quantified e.g. into an amount of available surface. This is in good agreement with well-established models. For example, Lynd *et al* [2] proposed that in amorphous cellulose there are much more regions available for EG I to depolymerize the substrate [15] and generate new chain ends. These can further be attacked by cellobiohydrolases.

### 2.3.2 CBH I

We applied the CBH I isolated from *T. longibrachiatum* towards both substrates. The time course of the Avicel hydrolysis is shown in Figure 1a, additionally the time course over the first five hours is emphasized in Figure 1b to provide a higher resolution of the initial points of the hydrolysis. The protein binding profile (Figure 3a) shows that the amount of bound protein per remaining mg substrate is decreasing over time. In spite of that, the amount of bound protein on our MAC substrate is first increasing and reached a stable state after 24 hours (Figure 3a). It is obvious that the conversion of the mainly amorphous and crystalline substrate is proceeding at a 10 % lower rate (compare Figures 1b and 2b). The calculated point of rate retardation can be pronounced for both substrates to be at 24 hours. After this time point, we observed no further conversion on the MAC substrate (Figure 2a). In contrast, we detected a low degree of conversion (6 % over the following 54 hours) on Avicel. The inverse protein binding profile (Figure 3a) might be a result of different amounts of surface available on our substrates. In fact the amount of available surface on Avicel could be estimated to be 10 fold higher in comparison to our MAC substrate [16]. We observed that the

initial amount of protein bound to Avicel is eight fold higher than the amount bound to the MAC substrate. This seems reasonable because CBH I is known to prefer crystalline substrates. However, the specific activity seems to be nine fold lower on the crystalline substrate (Table 1). This arises from the fact that only a low amount of enzyme is bound to the MAC substrate in the initial phase (eight fold less compared to Avicel). Furthermore the on the average 4.5 fold higher amount of enzyme bound on the MAC substrate indicates that a lot of CBH I is bound at unproductive positions on Avicel (Figure 3a). Another possibility is that the surrounding amorphous matrix influences the catalytic activity of CBH I. This could be supported by our AFM investigations, which showed that single fibrils are faster degraded than bundles of fibrils [manuscript in preparation].

Interestingly, we also observed that the amount of enzyme bound on the surface increase over time on the MAC substrate (Figure 3a). This might be a result of surface generation effects by enzymatic activity as previously reported by Bubner *et al* [12]. They could show that enzymes are able to modify the available amount of surface for instance by degrading objects below the surface plane.

Another interesting point is that the change of the amount of bound protein (Figure 3a) stops at the same time as the conversion (Figure 2a) after 24 hours. As we know from our AFM investigations our substrate provides fibril structures buried in or coated with an amorphous layer. Igarashi *et al* [17] showed that CBH I is not able to convert a fibril further once the enzyme is blocked by a steric hindrance. Those findings indicate that CBH I is trapped on the surface in unproductive binding positions e.g. on a fibril which cannot be further degraded due to the presence of overlaying amorphous substrate parts. This would lead to no further increase of the surface and moreover to a cease of the conversion.

In spite of that, we observed a release of bound protein over time on Avicel (Figure 3a) indicating that a significant amount of CBH I reached chain ends, thus being released from the substrate surface. Another interesting point is the observation of an increasing glucose share in the overall sugar pattern in the hydrolysis of Avicel (Figure 6). This effect was not observed on the MAC substrate overall. Usually CBH I produces mainly cellobiose [18]. There are, however, three possible explanations for the generation of glucose: first, a so called “false initial attack” [19] which propose that the first attack on a cellulose chain by CBH I could release aside from cellobiose also cellotriose or glucose, the hydrolysis of soluble cello-oligomers; and third, production of glucose by miscutting [20]. The ratio of glucose to cellobiose is reported to vary from a ratio of 1:7 up to 1:10 with Avicel as a substrate. However, studies on this matter did not use extended hydrolysis times (>48 hours). We find similar ratios up to 48 hours, with the described increase of glucose afterwards. This is most likely due to a larger amount of unbound CBH I available in the later phase of the hydrolysis (Figure 3a). These free enzymes might hydrolyse soluble cello-oligosaccharides originating from non-processive hydrolysis of the substrate to a certain extent. It was shown that especially the hydrolysis rate of cello-pentose would benefit from the increased amount of available enzyme since this reaction occurs slowly compared to the hydrolysis of cellotriose [21]. However there are clear indications that the ratio depends on the substrate properties as recently described by Kurasin *et al* [22]. CBH I seems to be more likely to perform miscutting on higher ordered substrates like Avicel than on the more amorphous phosphoric acid swollen cellulose (PASC).

### 2.3.3 CBH II

The time course of the enzymatic Avicel hydrolysis is shown in Figure 1a, where we observed a marked point of rate retardation after three hours. On the MAC substrate we detect the point of rate retardation after 12 hours. The overall conversion reaches a higher level on the MAC substrate (Figure 1a, 2a and Table 1). The protein binding profile (Figure 3b) shows different behavior on both substrates. On Avicel we saw an initial increase of bound protein and a release of bound protein after the point of rate retardation. In spite of that, we observed a steady increase of the amount of bound protein on the MAC substrate. This might be a result of the already mentioned higher amount of available surface on Avicel. The increase over time might arise from surface generation effects, which is in a good agreement with the ongoing conversion and the fivefold higher conversion compared to CBH I, where we assume surface generation effects also.

The specific activity (Table 1) indicates that CBH II prefers the mainly amorphous MAC substrate, which is further supported by the higher overall conversion. This is supported by molecular dynamic simulations showed how CBH II is able to undergo structural changes in the exo-loop regions which allow the enzyme to act as an endo-enzyme [23]. This provides CBH II with a clear advantage on amorphous substrates. Moreover, this might provide even an advantage on the microcrystalline substrate by introducing new chain ends in lower ordered parts resulting in an increase of bound protein (Figure 3b) as we observed it during the first three hours of the Avicel hydrolysis.

Another interesting observation is the decrease of bound protein on Avicel after the point of rate retardation. A possible explanation is that CBH II is able to leave binding positions if no further hydrolysis is possible. This is aggravated supported by our AFM data [manuscript in preparation].

### 2.3.4 EGI

Not unexpectedly, EGI shows the lowest conversion on the microcrystalline Avicel substrate (Figure 1a and Table 1). In spite of that, EG I showed a higher initial rate and a higher overall conversion after 24 hours on our MAC substrate (Figure 2a and Table 1). Interestingly, we observed on the MAC substrate, a significant initial lag phase (45 minutes) preceded by a tenfold increase of hydrolytic activity (Figure 2a and 2b). Moreover there is also a lag phase in terms of protein binding on the MAC substrate detectable (Figure 5). In contrast, we observed a steady increase of bound protein on Avicel (increased from 22 to 27  $\mu\text{g}/\text{mg}$  after 24 hours).

The effect of the initial lag phase during the conversion on the MAC substrate might be explained by the proposed mode of action of the EG I: randomly distributed introducing of chain ends does not lead to a soluble and detectable conversion product [2]. Later in the reaction, we observe a strong increase of conversion products, mainly glucose (Figure 6). The release of short carbohydrate products was previously reported by Karlsson *et al* [24] on soluble cellulose derivate (PASC and CMC). Even if those substrates are not fully comparable, there is a clear indication that EG I produce short gluco-oligosaccharides with a comparable loading of 14  $\mu\text{g}/\text{mg}$  substrate (Table 1).

Glucose or short gluco-oligosaccharides production might be explained by enzymatic crowding as recently seen by Liu *et al* [25]. This might cause these effects due to spatial proximity of enzymes. Moreover this effect was also observed using TrCel5A which also is an endoglucanase with a CBD produced by *Trichoderma sp.* showing a similar sugar profile as EG I [24].

Interestingly, we observed a lag phase in the protein binding profile over the same time span too (Figure 5). This indicates a connection between these effects (Figure 5). A possible

explanation might be that agglomeration as seen by Liu *et al* happens during this lag face leading to a fast binding and an increase of glucose production.

## 2.4 Conclusions

We could show that the whole cellulase system is more efficient in degrading amorphous cellulose than degrading crystalline cellulose. This could be derived from the overall lower activity of the single enzyme compounds (Table 1) on Avicel. Moreover, we observed a step like function during the initial phase of the MAC substrate (Figure 4) hydrolysis indicating that at least two different types of hydrolysis activities occur. One might be defined as surface preparation activity and the other activity as the cellulose degradation itself. This fits early results achieved on this substrate [12].

CBH I showed the highest initial rate of the probed single enzyme on the microcrystalline substrate (Table 1) but unexpectedly on the mainly amorphous MAC substrate too. Out of this we conclude that the activity of CBH I is not only depended on the degree of crystallinity but moreover from the matrix which embeds the crystalline fibrils.

Therefore the role of cooperative enzymes should be presumed in terms of making inaccessible regions available for CBH I either by revealing hidden chain ends or by introducing new chain ends. A step like function, which can be considered as a plateau (Figure 4), would be also support such a type of synergism in terms of two types of reaction following each other continuously until enough productive binding spots are available on the substrate.

Our results suggests that the role of CBH II needs to be rethought as that of a supportive enzyme which is able to reveal higher ordered regions coated by an amorphous layers which is supported by AFM analysis. In addition, there is a clear evidence for degrading amorphous

substrates at a higher rate (Table 1). Moreover, CBH II seems to be capable of leaving unproductive binding position, which was indicated in our Avicel hydrolysis study (Figure 1 and 3).

EG I showed strong binding on crystalline cellulose which does not result in a noticeable conversion (Table 1). Interestingly, the enzyme is capable of producing mainly glucose on the MAC substrate during the hydrolysis.

#### 2.4.1.1 Tables

**Table 1.** Comparisons of hydrolysis studies performed on different substrates. (\* not detectable due to low overall conversion rate)

		SVG17	CBH I	CBH II	EG I
Avicel Hydrolysis	Enzyme loading [ $\mu\text{g}/\text{mg}$ substrate]	3.6	36	420	36
	Point of rate retardation [h] <sup>I</sup>	24	24	3	n.d. *
	highest Conversion [%]	$53 \pm 0.1$	$19 \pm 0.2$	$13 \pm 0.5$	2.5
	Conversion at rate retardation [%]	$42 \pm 0.5$	$12 \pm 0.2$	$11 \pm 0.2$	$2.5 \pm 0.3$
	Initial rate [ $\mu\text{mol mg}_{\text{enzym}}^{-1} \text{h}^{-1}$ ] <sup>II</sup>	230	4.1	2.3	0.2
MAC Hydrolysis	Enzyme loading [ $\mu\text{g}/\text{mg}$ substrate]	3.6	36	420	36
	Point of rate retardation [h]	24	24	12	24
	highest Conversion [%]	$88 \pm 0.1$	$14 \pm 0.3$	$58 \pm 1.4$	$60 \pm 0.1$
	Conversion at rate retardation [%]	$69 \pm 1.9$	$12 \pm 0.3$	$49 \pm 1.3$	$48 \pm 0.2$
	Initial rate [ $\mu\text{mol mg}_{\text{enzym}}^{-1} \text{h}^{-1}$ ]	840	37	9.5	$8.1^{\text{II}}/22.6^{\text{III}}$

<sup>I</sup>: This point is reached from then on the hydrolysis rate drops below 15 % of the initial rate.

<sup>II</sup>: Initial rate was calculated using the released reducing sugars during the first hour of our hydrolysis studies according to Equation 1.

<sup>III</sup>: Initial rate was calculated in the first two hours after the lag phase.

### 2.4.1.2 Figures

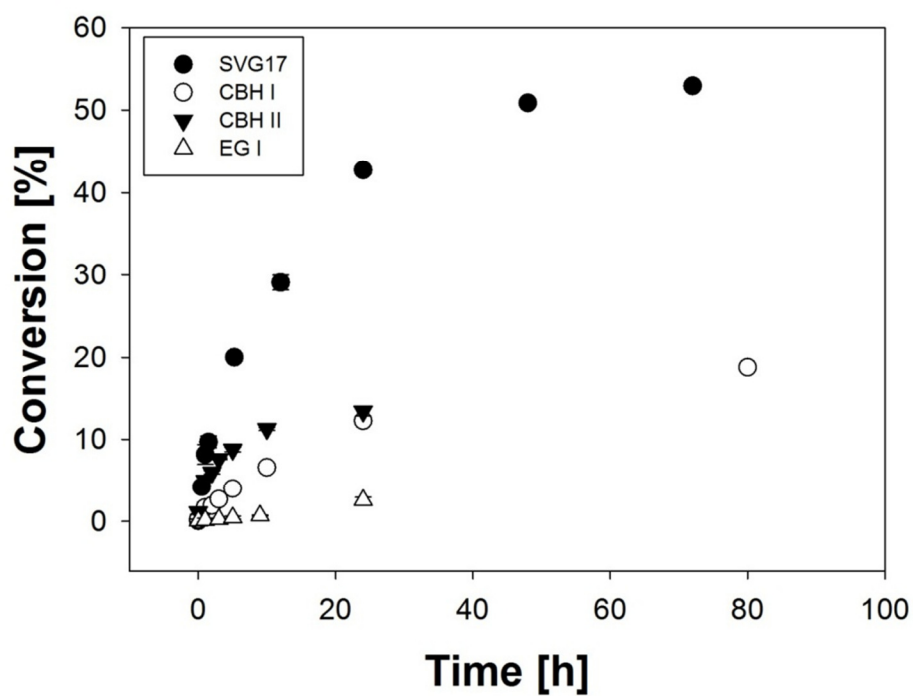


**Figure 1a.** Conversion profiles of single cellulolytic enzymes probed towards Avicel. Conversion is calculated as the amount of released reducing sugars calculated as anhydroglucose. Loadings used were 3.6  $\mu\text{g}/\text{mg}$  for SVG17, 36  $\mu\text{g}/\text{mg}$  for CBH I, 36  $\mu\text{g}/\text{mg}$  for EG I and 420  $\mu\text{g}/\text{mg}$  for CBH II according to Table 1.

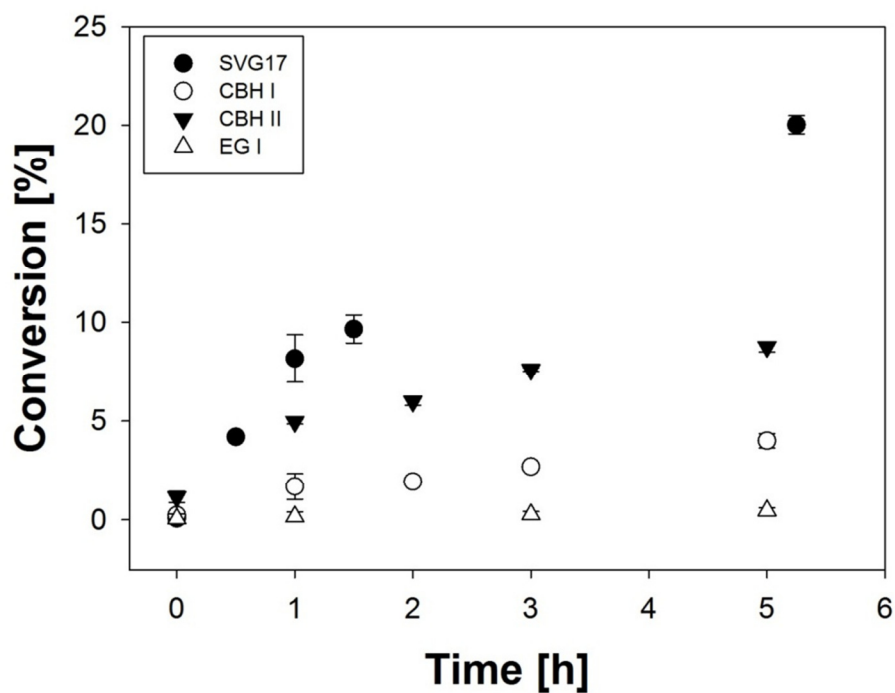


**Figure 1b.** Conversion profiles of single cellulolytic enzymes probed towards Avicel over the initial five hours. Conversion is calculated as the amount of released reducing sugars calculated as anhydroglucose. Loadings used were 3.6  $\mu\text{g}/\text{mg}$  for SVG17, 36  $\mu\text{g}/\text{mg}$  for CBH I, 36  $\mu\text{g}/\text{mg}$  for EG I and 420  $\mu\text{g}/\text{mg}$  for CBH II according to Table 1.

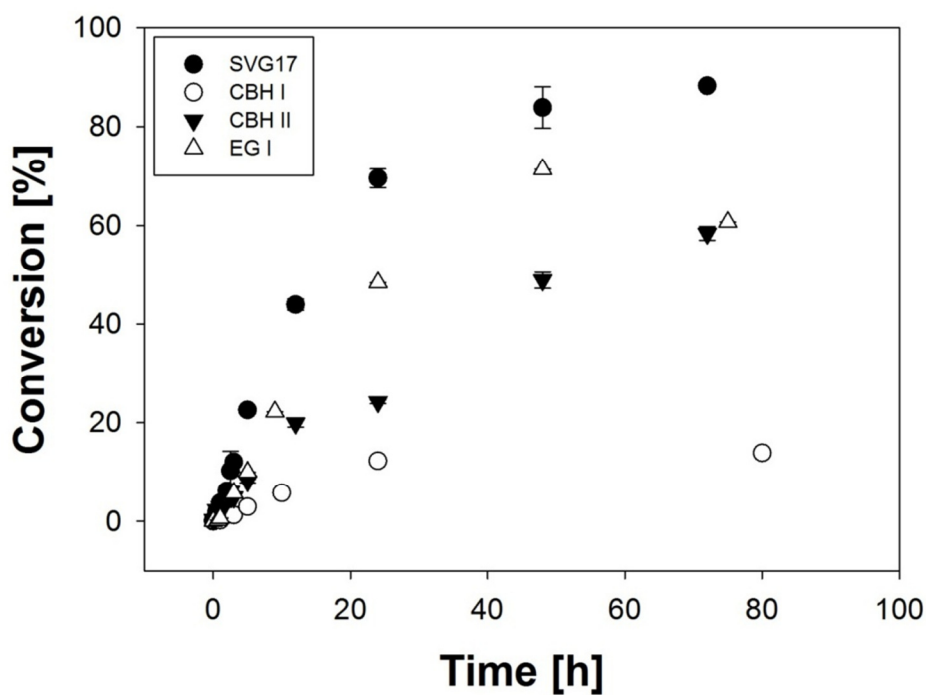


**Figure 2a.** Conversion profiles of single cellulolytic enzymes probed towards our MAC substrate. Conversion is calculated as the amount of released reducing sugars calculated as anhydroglucose. Loadings used were 3.6  $\mu\text{g}/\text{mg}$  for SVG17, 36  $\mu\text{g}/\text{mg}$  for CBH I, 36  $\mu\text{g}/\text{mg}$  for EG I and 420  $\mu\text{g}/\text{mg}$  for CBH II according to Table 1.

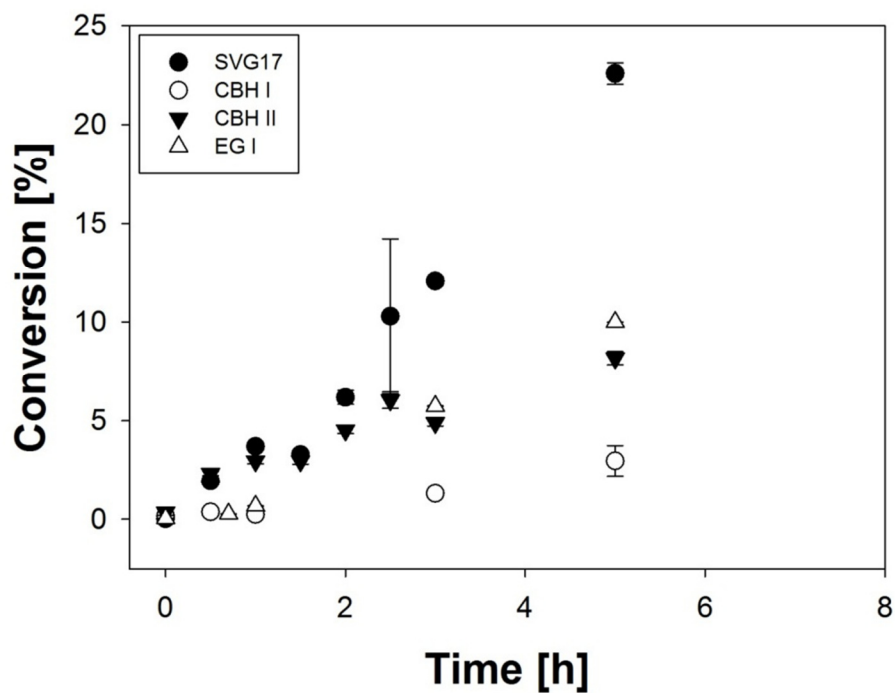


**Figure 2b.** Conversion profiles of single cellulolytic enzymes probed towards our MAC substrate over the initial five hours. Conversion is calculated as the amount of released reducing sugars calculated as anhydroglucose. Loadings used were 3.6  $\mu\text{g}/\text{mg}$  for SVG17, 36  $\mu\text{g}/\text{mg}$  for CBH I, 36  $\mu\text{g}/\text{mg}$  for EG I and 420  $\mu\text{g}/\text{mg}$  for CBH II according to Table 1.

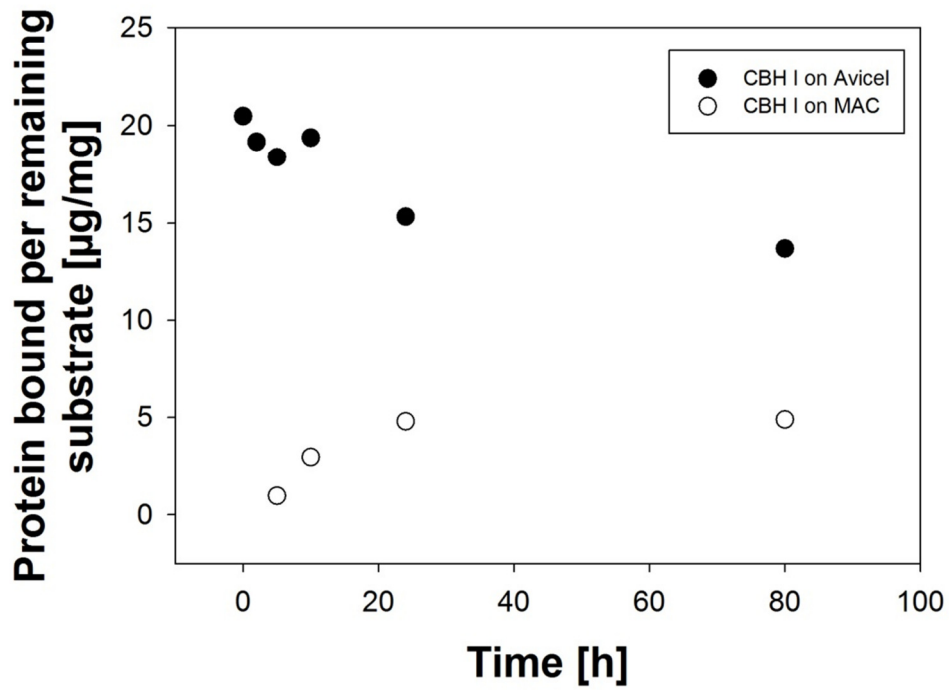


**Figure 3a.** Time course analysis for protein adsorption calculated for CBH I based on the remaining amount of substrate. Interestingly, we observed an inverse behaviour on our substrates.

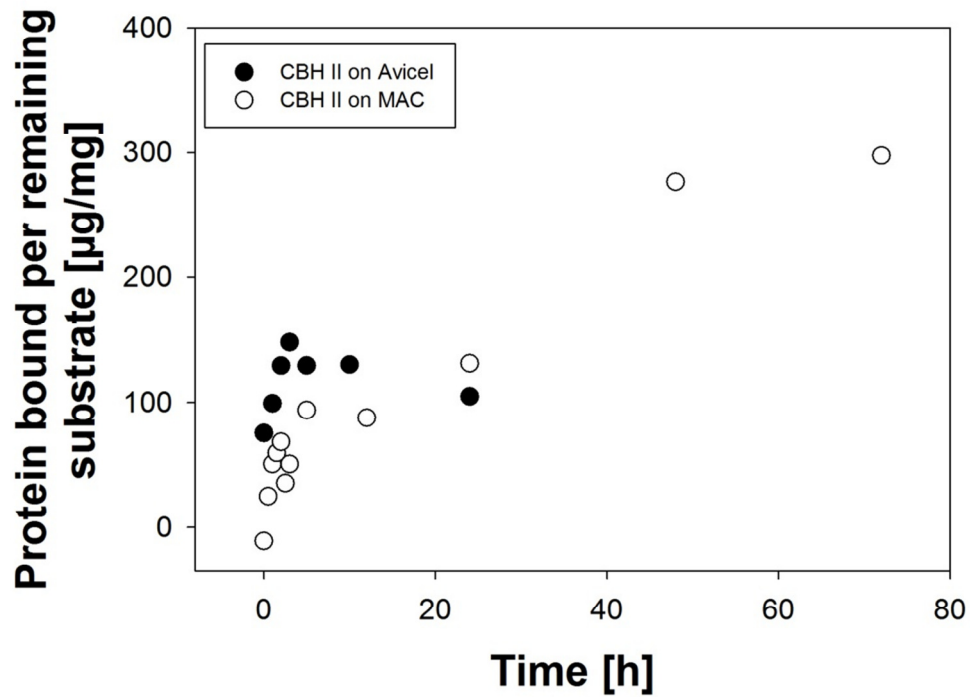


**Figure 3b.** Time course analysis for protein adsorption calculated for CBH II based on the remaining amount of substrate. It is obvious that the amount of protein bound on the MAC substrate increase over time with a plateau after 10 hours preceded by further adsorption after 20 hours. In spite of that, we observed on Avicel a release of bound protein after five hours.

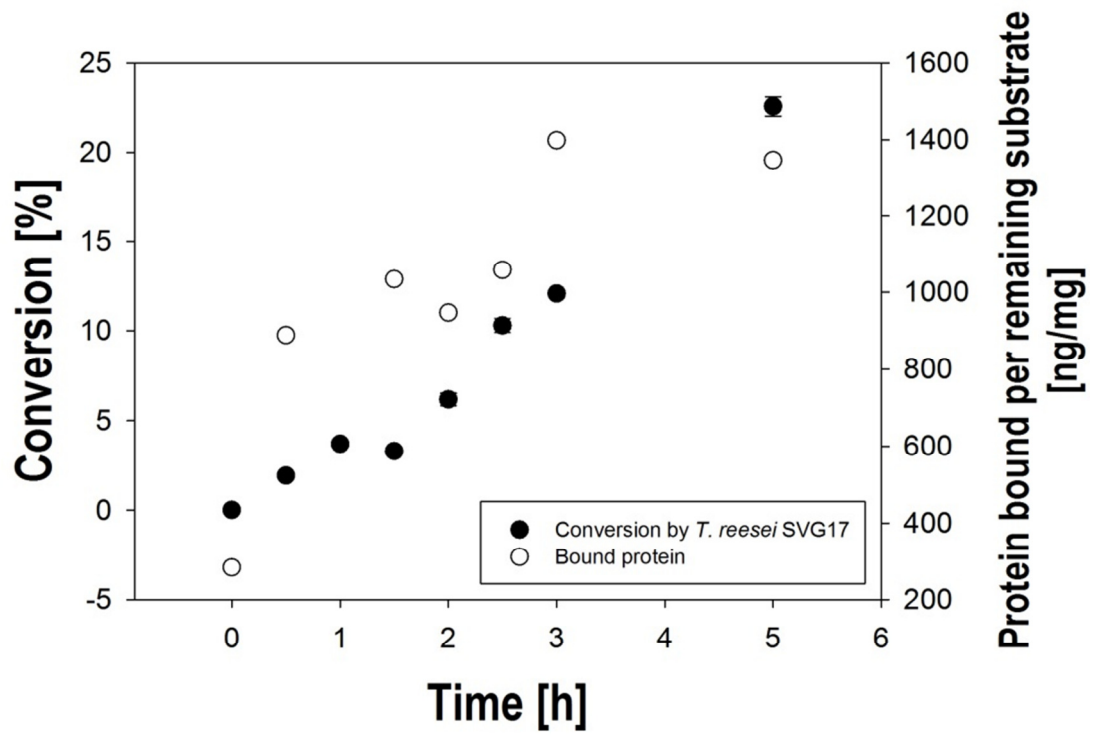


**Figure 4.** Step like kinetic behaviour was observed for both hydrolysis and protein adsorption during the degradation of the MAC substrate by *T. reesei* SVG17 over the first five hours.

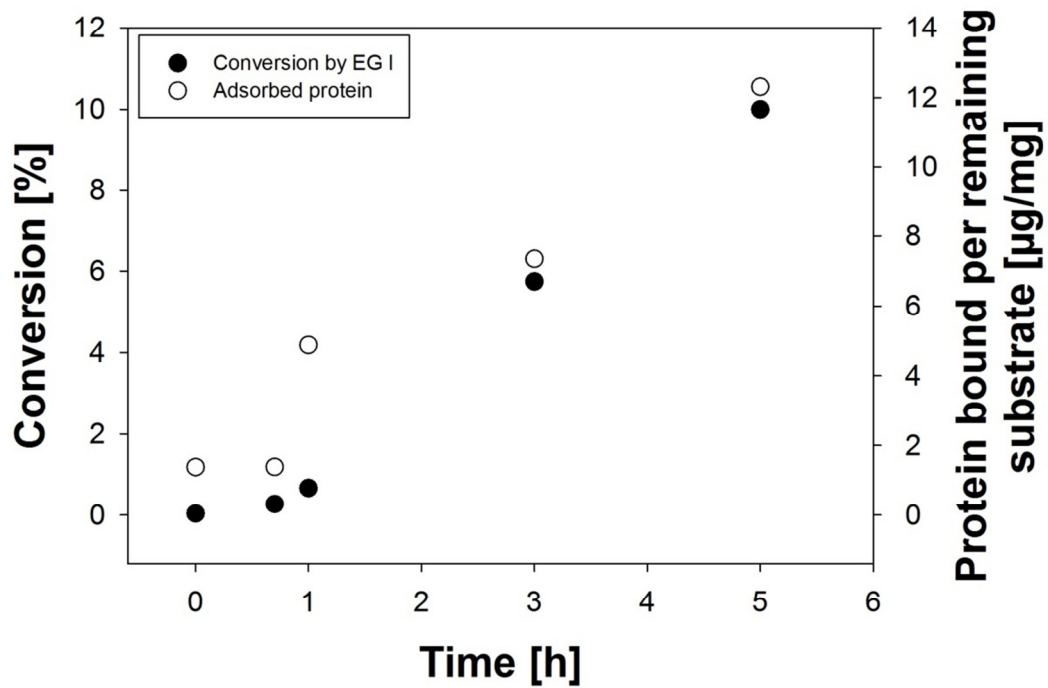


**Figure 5.** A lag phase was observed for both hydrolysis and protein adsorption during the degradation of the MAC substrate by EG I during the first 45 minutes. Afterwards there is a simultaneous increase of both kinetic parameters detectable.

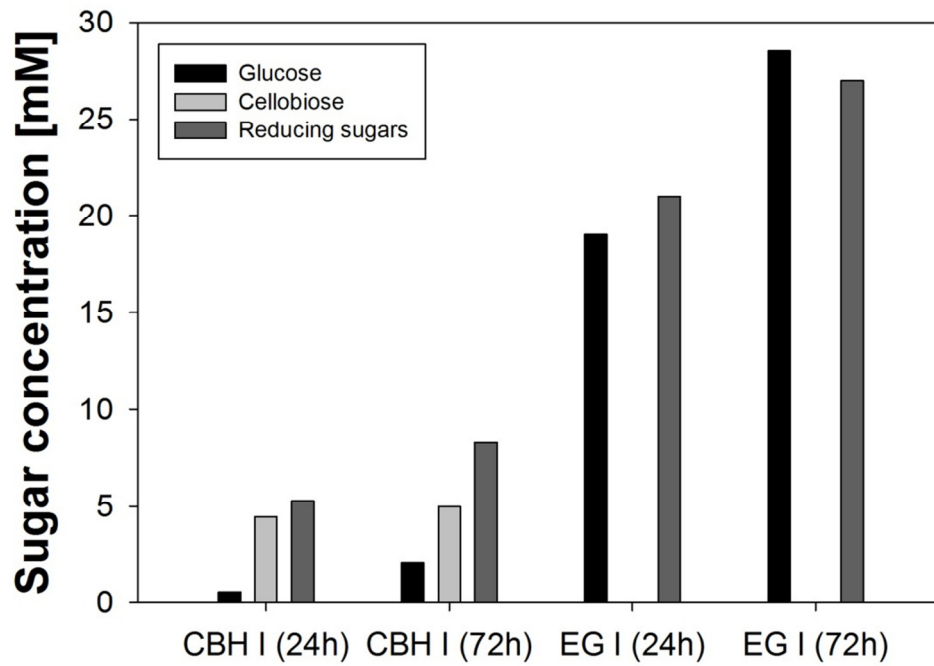


**Figure 6.** Sugar profile of the Avicel hydrolysis of CBH I showing a clear increase of glucose after 24 hours. The sugar profile of EG I during the MAC hydrolysis clearly shows the formation of glucose.

## 2.5 References

- [1] Lynd L. R., Laser M., Bransby D., Dale B., Davison B., Hamilton R., Himmel M., Keller M., McMillan J., Sheehan J. and Wyman C. (2008) How biotech can transform biofuels. *Nature Biotechnology* **36**, 169-72
- [2] Lynd L. R., Weimer P. J., Van Zyl W. H. and Pretorius I. S. (2002) Microbial cellulose utilization: fundamentals and biotechnology. *Microbiology and Molecular Biology Reviews* **66**, 506–577
- [3] Chundawat S., Bellesia G., Uppugundla N., Susa L., Gao D., Cheh A., Agarwal U., Bianchetti C., Langan G., Venkatesh B., Gnanakaran S. and Dale B. (2011) Restructuring the crystalline cellulose hydrogen bond network enhances its depolymerization rate. *Journal of the American Chemical Society* **133**, 11163-74
- [4] Bansal P., Hall M., Realff M. J., Lee J. H. and Bommarius A. S. (2009) Modeling cellulase kinetics on lignocellulosic substrates. *Biotechnology Advances* **27**, 833-48
- [5] Fagerstam L. G. and Pettersson L. G. (1980) The 1,4- $\beta$ -glucan cellobiohydrolases of *Trichoderma reesei* QM 9414: A new type of cellulolytic synergism. *FEBS Letters* **119**, 97–100
- [6] Kleywegt G., Zuo J., Divne C., Davies G., Sinning I., Stahlberg J., Reinikainen T., Srisodsuk M., Teeri T. and Jones T. (1997) The crystal structure of the catalytic core domain of endoglucanase I from *Trichoderma reesei* at 3.6 Å resolution, and a comparison with related enzymes. *Journal of Molecular Biology* **272**, 383-97
- [7] Liu Y., Luo Y., Baker J. and Zeng Y. (2010) A single molecule study of cellulase hydrolysis of crystalline cellulose. *Society of Photo-Optical Instrumentation Engineers, Conference Paper NREL/CP-270-47301*
- [8] Liu Y.-S., Baker J. O., Zeng Y., Himmel M. E., Haas T. and Ding S.-Y. (2011) Cellobiohydrolase hydrolyzes crystalline cellulose on hydrophobic faces. *Journal of Biological Chemistry* **286**, 11195-201
- [9] Prasad K., Kaneko Y. and Kadokawa J. (2009) Novel gelling systems of kappa-, iota- and lambda-carrageenans and their composite gels with cellulose using ionic liquid. *Macromolecular Bioscience* **9**, 376-82
- [10] Esterbauer H., Steiner W., Labudova I., Hermann A. and Hayn M. (1991) Production of *Trichoderma* cellulase in laboratory and pilot scale. *Bioresource Technology* **36**, 51-65

- [11] Compton S. and Jones C. (1985) Mechanism of dye response and interference in the Bradford protein assay. *Analytical Biochemistry* **151**, 369-374
- [12] Bubner P., Dohr J., Plank H., Mayrhofer C. and Nidetzky B. (2011) Cellulases dig deep: in situ observation of the mesoscopic structural dynamics of enzymatic cellulose degradation. *Journal of Biological Chemistry*, accepted November the 29<sup>th</sup>, 2011
- [13] Xiao Z., Storms R. and Tsang A. (2004) Microplate-based filter paper assay to measure total cellulase activity. *Biotechnology and Bioengineering* **88**, 832-7
- [14] Park S., Baker J. O., Himmel M. E., Parilla P. and Johnson D. K. (2010) Cellulose crystallinity index: measurement techniques and their impact on interpreting cellulase performance. *Biotechnology for Biofuels* **3**:10
- [15] Griggs A. J., Stickel J. J. and Lischeske J. J. (2011) A mechanistic model for enzymatic saccharification of cellulose using continuous distribution kinetics I: Depolymerization by EG I and CBH I. *Biotechnology and Bioengineering*, accepted September 26<sup>th</sup>, 2011
- [16] Ek R. and Alderborn G. (1994) Particle analysis of microcrystalline cellulose: differentiation between individual particles and their agglomerates. *International Journal of Pharmaceutics* **111**, 43-50
- [17] Igarashi K., Uchihashi T., Koivula A., Wada M., Kimura S., Okamoto T., Penttilä M., Ando T. and Samejima M. (2011) Traffic jams reduce hydrolytic efficiency of cellulase on cellulose surface. *Science* **333**, 1279-1282
- [18] Zhao X., Rignall T. R., McCabe C., Adney W. S. and Himmel M. E. (2008) Molecular simulation evidence for processive motion of *Trichoderma reesei* Cel7A during cellulose depolymerisation. *Chemical Physics Letters* **460**, 284-288
- [19] Medve J., Karlsson J., Lee D. and Tjerneld F. (1998) Hydrolysis of microcrystalline cellulose by cellobiohydrolase I and endoglucanase II from *Trichoderma reesei*: adsorption, sugar production pattern, and synergism of the enzymes. *Biotechnology and Bioengineering* **59**, 621-34
- [20] Nidetzky B., Zachariae W., Gercken G. and Hayn M. (1994) Hydrolysis of ceiloooligosaccharides by *Trichoderma reesei* cellobiohydrolases: Experimental data and kinetic modelling. *Enzyme and Microbial Technology* **16**, 43-52
- [21] Vrsanska M. and Biely P. (1992) The cellobiohydrolase I from *Trichoderma reesei* QM 9414: action on cello-oligosaccharides. *Carbohydrate Research* **227**, 19-27
- [22] Kurasin M. and Väljamäe P. (2011) Processivity of cellobiohydrolases is limited by the substrate. *Journal of Biological Chemistry* **286**, 169-77

- [23] Zou J., Kleywegt G., Stahlberg J., Driguez H., Nerinckx W., Claessens M., Koivula A., Teeri T. and Jones A. (1999) Crystallographic evidence for substrate ring distortion and protein conformational changes during catalysis in cellobiohydrolase Cel16A from *Trichoderma reesei*. *Structure* **7**, 1035-45
- [24] Karlsson J., Siika-aho M., Tenkanen M. and Tjerneld F. (2002) Enzymatic properties of the low molecular mass endoglucanases Cel12A (EG III) and Cel45A (EG V) of *Trichoderma reesei*. *Journal of Biotechnology* **99**, 63-78
- [25] Liu H., Fu S., Zhu J. Y., Li H. and Zhan H. (2009) Visualization of enzymatic hydrolysis of cellulose using AFM phase imaging. *Enzyme and Microbial Technology* **45**, 274-281

### 3 Appendix A –Real time observation of enzymatic cellulose degradation

#### 3.1 Introduction

Over the last decades, researchers have investigated cellulolytic activity using a combination of various biochemical assays and different types of imaging techniques such as fluorescence microscopy, transmission electron microscopy (TEM) and scanning microscopy (SEM) [1]. Electron beam based techniques have several disadvantages like complex sample preparation, influencing sample structure and inability to provide in situ information.

With the upcoming of atomic force microscopy in the 1980s arose different new opportunities to measure in situ real-space three-dimensional data and also the possibility to achieve information about surface properties like mechanical stability or electrostatic potential [2].

This all is possible under physiological conditions – in air or liquid. Moreover commercial AFM software allows for different ways to achieve statistical data of image sets like the change of the average surface roughness.

Studies of cellulose-and cellulases on a molecular level provide us with a deeper insight of what single cellulolytic enzymes are actually doing on substrates. A few of those studies have been performed using atomic-force-microscopy [3], [4]. From these studies we received important insights into the mode of action of CBH I on crystalline substrates e.g. a stop and go like motion motive on fibril like structures [5], [6].

In our work we focused on the single enzyme compounds of the fungal cellulolytic system of different *Trichoderma* strains using the advantage of having a MAC substrate providing crystalline and amorphous parts. Previous AFM studies were limited in that they employed

strictly crystalline substrates such as algal cellulose. Moreover we were able to give a mesoscopic view on what is actually happening on the surface looking on a considerably larger part. We chose different enzyme loading and proper reaction conditions to achieve a better resolution of the single cellulolytic activities.

Our investigations resulted in a movie showing the synergistic degradation of cellulose leading to new insights about the role of single enzymes in a typical fungal cellulase system [7].

## 3.2 Material and Methods

### 3.2.1 Materials

Citric acid, sodium citrate and sodium hydroxide were purchased from Carl Roth, Karlsruhe, Germany. Avicel PH-101 and 1-butyl-3-methylimidazolium chloride (BMIMCl) were obtained from Sigma-Aldrich, Vienna, Austria. Sodium potassium tartrate, phenol and 3,5-dinitrosalicylic acid (DNS) was purchased from Merck, Vienna, Austria.

### 3.2.2 Enzyme preparation

CBH I and EG I (isolated from *T. longibrachiatum*) were obtained from Megazyme International, Dublin, Ireland and stored until further use by 4 °C. The lyophilisate of CBH II (protein sequence [Supporting Information 6.1]) isolated from *T. reesei* and expressed in *P. pastoris* was a gift of the Institute of Molecular Biotechnology (Graz University of Technology) and stored until further use by – 20 °C. Before use the enzymes were subjected to buffer exchange using a NAP-25 columns purchased from GE Healthcare, Vienna, Austria. Buffer exchange was performed according to the manufactures protocol.

The complete cellulase system from *Trichoderma reesei* SVG17 was produced as described by Esterbauer *et al.* [8] and supplemented with 0.05 % sodium azide for storage at 4 °C. Protein concentration was determined to be 0.48 g/l using a “Bovine Serum Albumin” (BSA) calibrated Bradford Assay [9]. Activity was determined, as recommended by IUPAC, using the well established “filter paper units” (FPU) assay [8]. According to this assay, our cellulase system had 1.0 FPU/ml.

### 3.2.3 Atomic force microscope (AFM)

We used a commercial Dimension 3100 AFM equipped with a Hybrid scanner and Nanoscope IVa controller from Bruker AXS, Santa Barbara, Canada for all AFM measurements. We performed the imaging in tapping mode to avoid influencing the enzymes on the surface by constant tip contact.

The measurements were performed in a self-developed sample holder (Figure 1) using  $3.0 \pm 0.5$  ml of 50 mM sodium citrate buffer at pH 5.0 at a temperature of 20 °C. We exposed 0.5 mg MAC substrate to enzyme loadings according to our hydrolysis studies. The reactions were imaged using AFM according to the enzymatic activity applied to yield a good resolution of the degradation over time but for at least three hours.

### 3.2.4 AFM image analyses

We performed detailed image analysis using the software packages Research Nanoscope V7.20 (Bruker, AXS, Santa Barbara, Canada) to quantify observed features and confirm extracted data.

We extracted data describing the changing topology of the overall substrate surface, i.e. root-mean-squared (RMS) surface roughness and phase images providing information about the

mechanical properties of the surface. So we were able to distinguish between crystalline and amorphous regions.

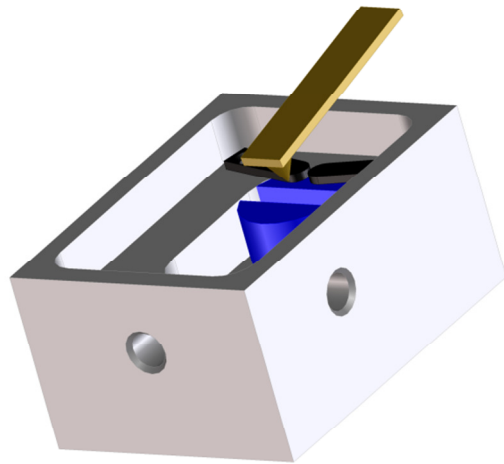


**Figure 1.** Blueprint of our self-developed sample holder (image courtesy of Thomas Ganner) used for our AFM studies. The epoxy embedded gel was placed in the cavity of the blue aluminium formed retainer afterwards the liquid cell indicated by the golden cantilever was approached via the AFM software.

### 3.2.5 Preparation of the model substrate

The substrate was prepared according to Prasad *et al* [10] by dissolving 0.13 g Avicel PH-101 (i.e. 13 % w/w) in 1.0 g BMIMCl by heating at 100 °C for 24 hours with stirring in an air condition controlled room at 23 °C. Secondly, we cut this so called primary gel into squares with a side length of approximately 5 mm and an average thickness of 250  $\mu\text{m}$ . Afterwards the solvent and loosely bound water molecules were removed using a fractionated ethanol extraction protocol (stepwise increase from 30 % to absolute ethanol). Following these

secondary gels were air-dried and analyzed using STA and XRD analysis to confirm purity and present cellulose allomorphs as described previously by Bubner *et al* [3].

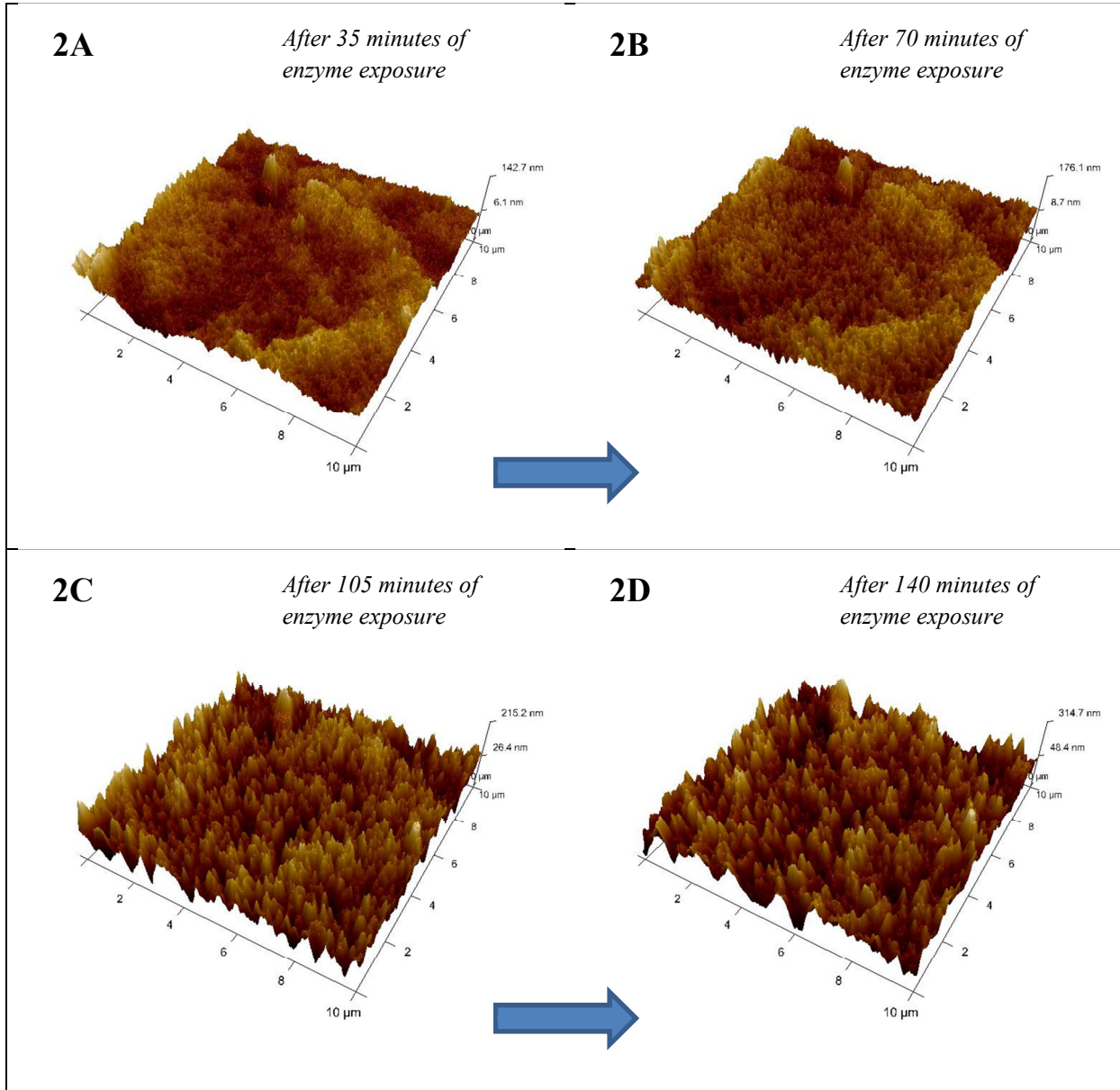
Before our AFM investigations the MAC substrate was embedded in epoxy-resin and treated with an ultra-microtome leading a surface with an average roughness of less than 15 nm.

### 3.3 Results and Conclusion

#### 3.3.1 SVG17

After applying the whole supernatant we observed a lag phase of approximately 1h. This reproducible phenomenon could be observed by other probed enzymes too. Thus, we assume that this effect arises from diffusion limitation by conditions of 20 °C. Additional cellulases are known to use only a lateral diffusion mode and in the presence of a cavity (Figure 1) on our sample holder this lead to further delay until enzymes reaches the substrate.

After the lag phase we observe a massive attack of our substrate in terms of a loss of volume which can be measured through changes in the height profile. In a section image regarding the height information we observed an extensive, constant decomposition of the surface with the exception of the highly order crystalline part (Figure 3). Consequently, we used such crystalline inclusion bodies for all other experiments as position marker since the whole supernatant was not able to attack them.



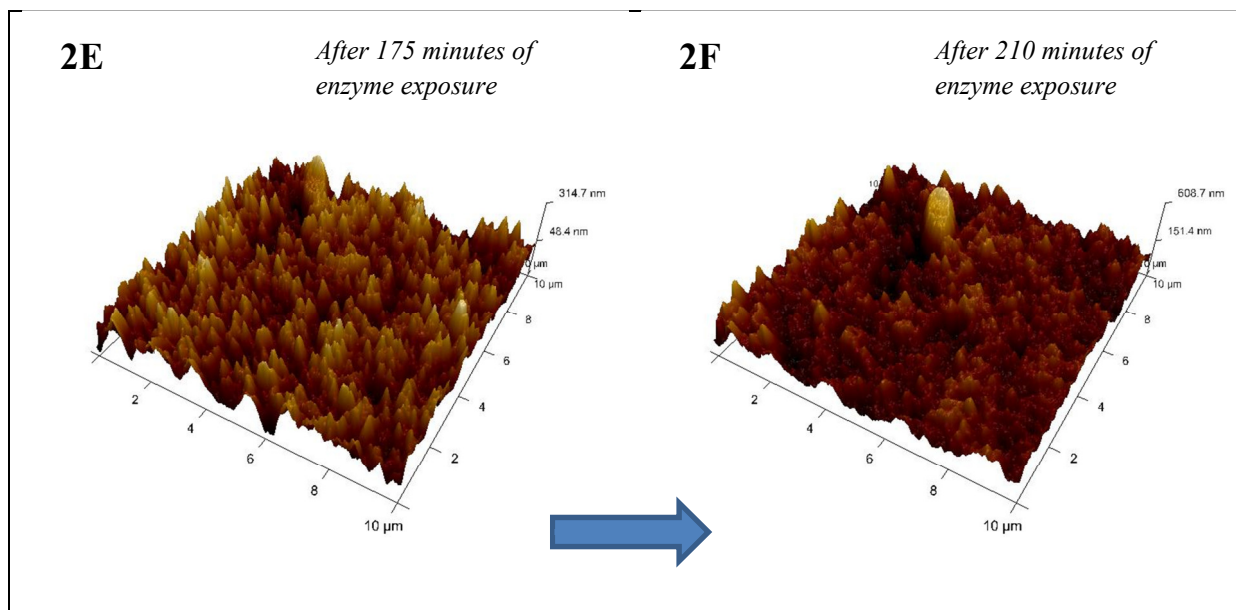


**Figure 2.** This image series shows the large scale degradation of our substrate performed by the whole fungal cellulase system produced by *T. reesei* SVG17 over a time span of approximately three hours. The height information is reflected in these three-dimensional images and phase information is reflected in the colour of the surface. Brighter parts are more crystalline than the darker, amorphous parts. We used a crystalline inclusion body for orientation which is best seen in the lower upper centre of the Figure 2F.

Interestingly, the degradation of amorphous parts occurs faster leading to an increase of crystalline parts mainly on top of small exaltations. After some delay, these structures are also attacked and degraded rapidly. Eventually, only the previously mentioned inclusion body was left surmounting the plane. This was also observed in the section profile, which reflects the change of distinct points along the overall surface with time (Figure 2 and 3). Interestingly, the degradation of amorphous material happens continuously increasing the amount of crystalline regions (e.g. Figure 2A up to 2C) available. In spite of that, the degradation of crystalline parts occurs discontinuously (e.g. Figure 2E and 2F). Out of this we conclude that the degradation of our MAC substrate proceeds in two steps. During the first step amorphous

material is removed. Allowing the enzymes, mainly CBH I, to degrade crystalline material at a higher efficiency in the second step. This is in good agreement with earlier studies concerning this substrate [3].

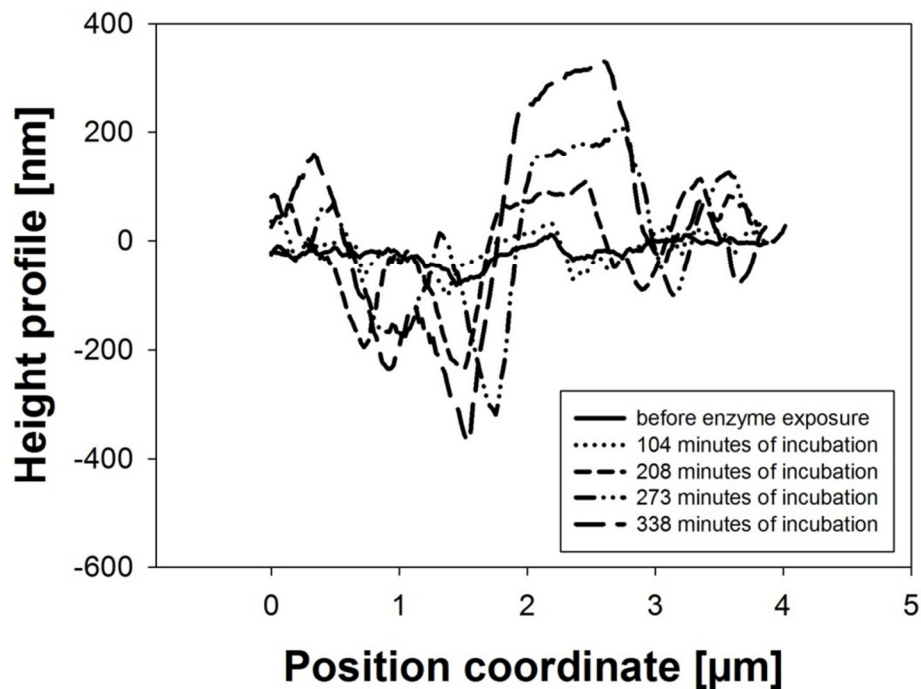


**Figure 3.** A clear change in the height profile was detectable after exposing the MAC substrate to the complete cellulase system. A crystalline inclusion body (located at the position coordinates 2-3  $\mu\text{m}$ ) was used as reference point. Interestingly, there seems to be an increase of the relative hydrolysis rate over time. Interestingly, we observed that the relative rate of the surface degradation increased over time.

When using a smaller scan size with a side length of 500 nm we are able to observe fibril like structures located on the surface. These structures seem to be higher ordered as the

surrounding area based on the overlaid phase image data (Figure 4). It is also visible that some of these fibrils are coated with amorphous material. Some of the fibrils are oriented in a different way relative to the plane. These structural features - crystalline material hidden or coated by amorphous material - are a key feature of our substrate.

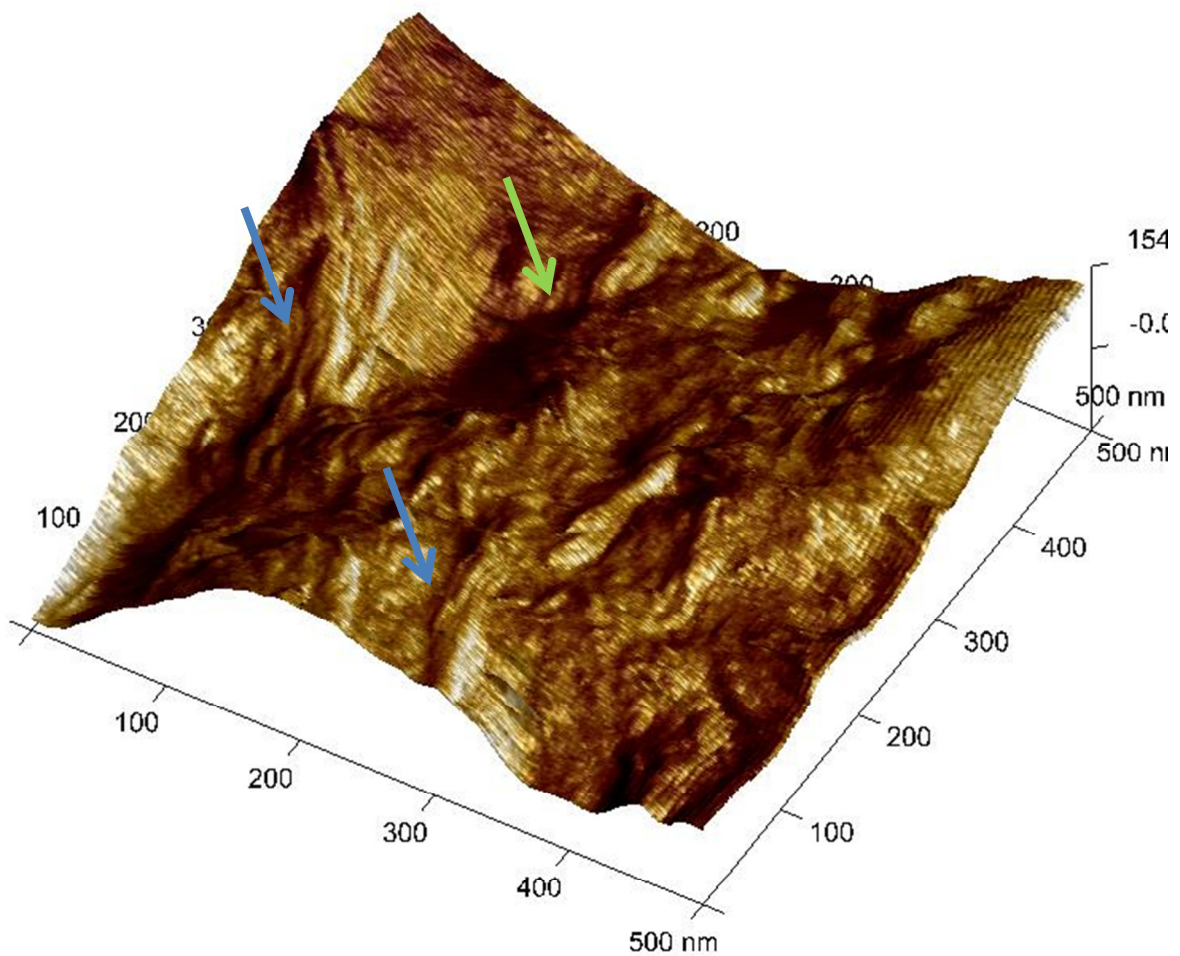


**Figure 4.** A detailed topographical image overlaid with phase information (by colour) of our substrate. Fibril like structures in different orientation (indicated by blue arrows) can be

clearly seen distributed on the surface. Some of them are at least partially covered with amorphous material (green arrow).

After a lag phase of one hour, we observed a relative rapid attack of our substrate. The degradation can be classified in different types: volume degradation is measurable through changes in the height images and through several structural changes on the surface. Examples for these structural changes are variances in the phase information or the degradation respectively formation of new structures on the surface. Fibrils are degraded mainly towards one end. However, starting from defects occurring within these fibril like structures, degradation always proceeded towards both ends (Figure 5). Strikingly, we did not observe a decrease in fibril width at all.

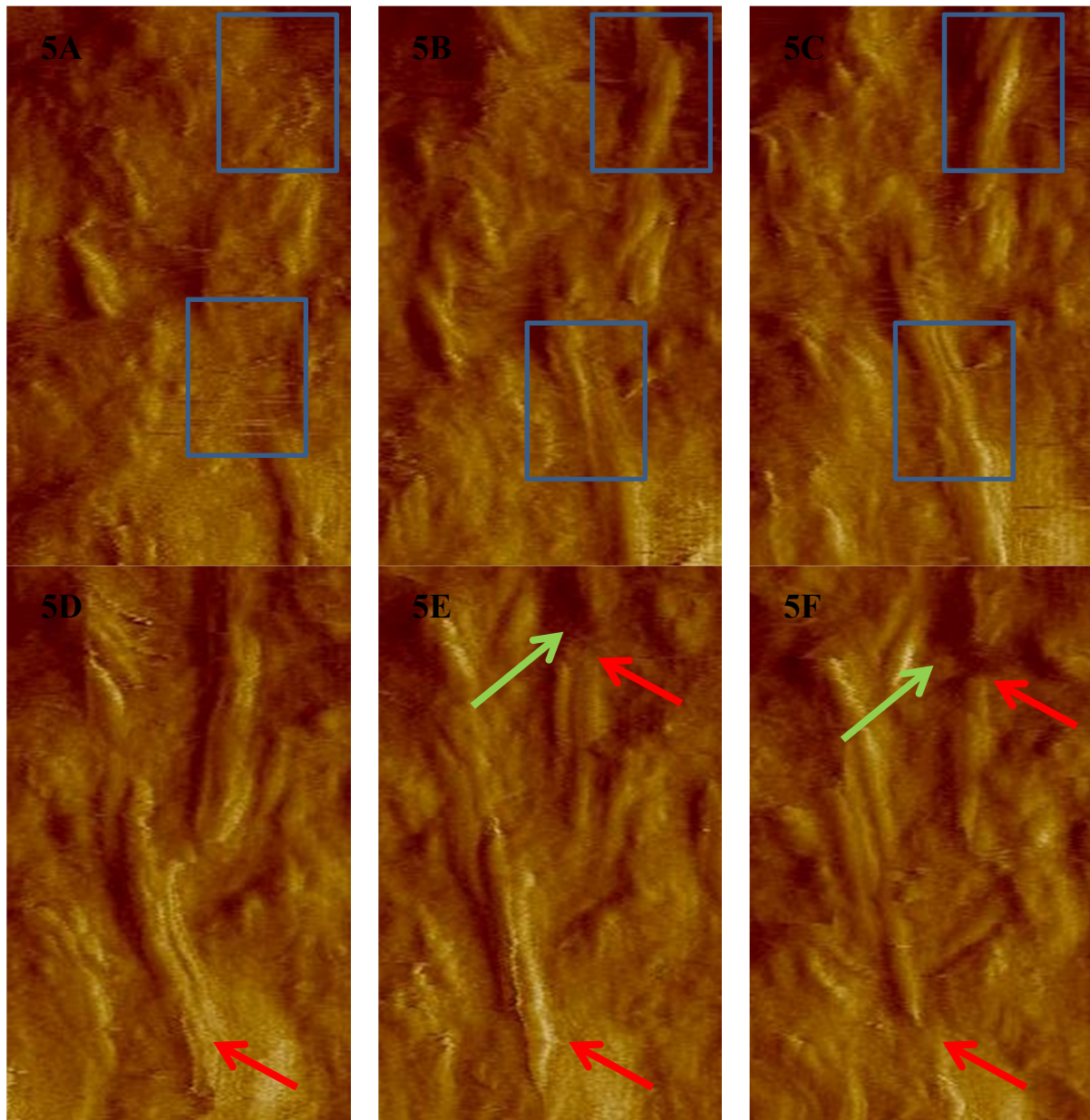


**Figure 5.** Detailed process of removing amorphous material until fibrils are completely accessible (blue squares) by enzymes resulting in a mainly unidirectional degradation (red arrows). Further we could observe the introduction of defects within fibrils (green arrows). The shown degradation process was recorded over one hour. According to this, a representative image was chosen every ten minutes.

The interpretation of these structural changes is done in the following based on the common knowledge of what single enzymes of the fungi supernatant are actually doing supported by our own analytical data. A sequence of AFM images was compiled to create a real time visualization of enzymatic cellulose degradation. The loss of volume is caused mainly by degradation of amorphous parts, a task assigned to EG I and CBH II. It should be stated, however, that these enzymes employ a different mode of action to remove volume and release structurally tighter packed parts. EG I might be also responsible for the introduction of structural defects within the fibrils which Liu et al. [11] observed as well in their study. The degradation of the crystalline fibrils itself is mainly performed by CBH I according to our data and what is known from literature [12], [13]. From this we propose a new type of exo-endo-based synergism. This model is characterized by two main activities: the first one being basically responsible for removing amorphous parts to make crystalline parts accessible. The second one is responsible for degrading these revealed crystalline regions. We identify CBH II and EG I as contributors to the first group. CBH II is able to attack crystalline areas but is limited in converting them. Our experiments indicate that CBH I is the main force acting on crystalline substrate parts.

### 3.3.2 CBH I

CBH I is well described in literature as the cellulase with a strong preference for crystalline cellulose [14]. Therefore we expected to see a rapid attack of all available crystalline structures. In our study, we observe only small changes in the average surface roughness in a wave like function (Figure 6). This indicates the occurrence of so called “surface regeneration effects: This means that crystalline parts above the plane get degraded slowly, thereby decreasing the surface until those parts are in the plane. Afterwards the degradation continues

until those parts are degraded completely and holes are left in the plane, thus increasing the average roughness again.

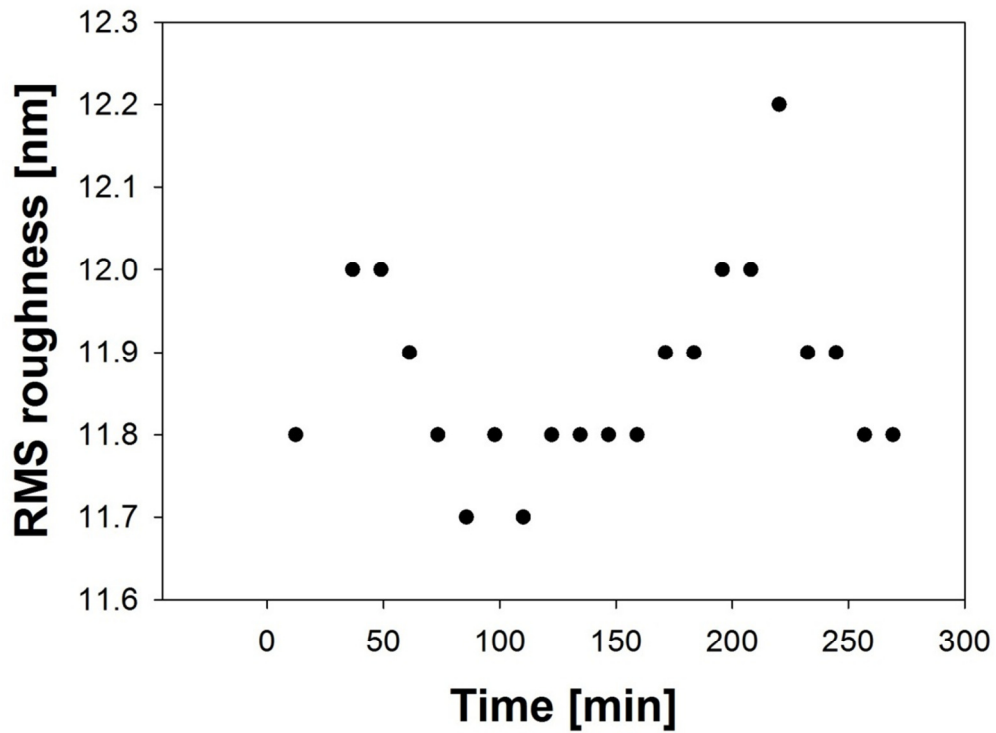


**Figure 6.** The average roughness of the surface calculated over a statistical relevant part of the surface excluding inclusion bodies.

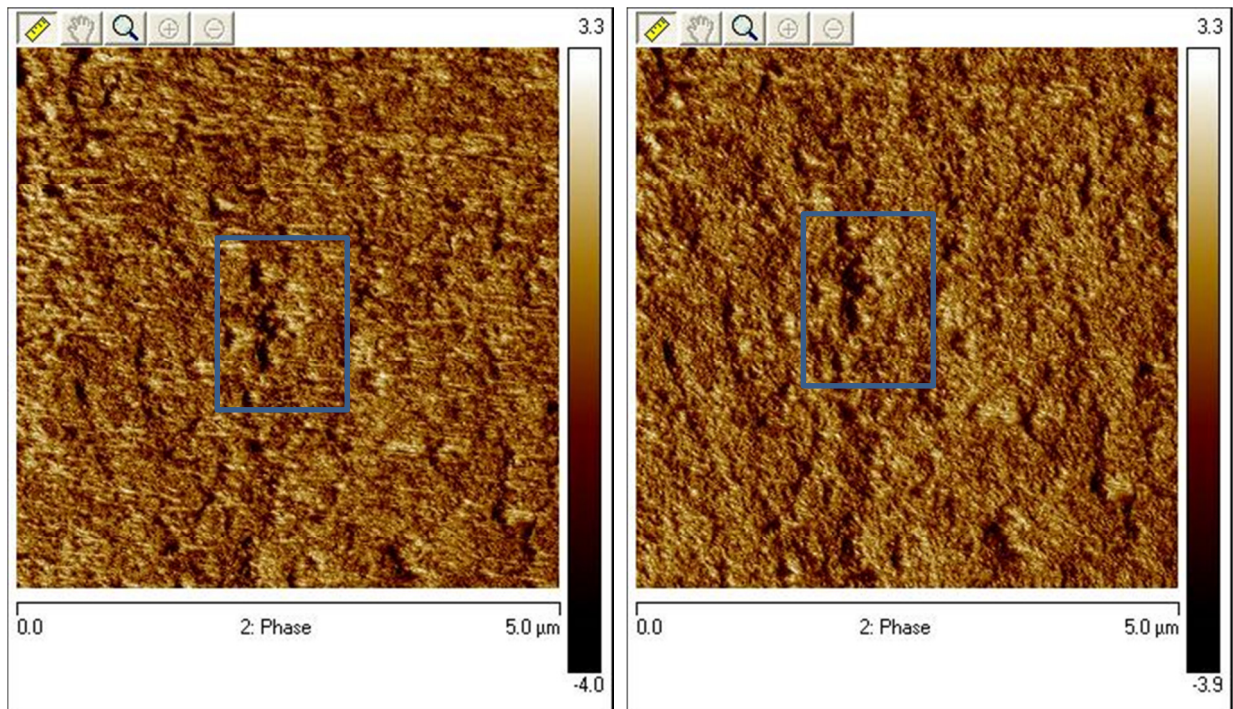


**Figure 7.** Comparison of two phases images collected before (left side) and after 245 minutes of incubation with CBH I. Mainly small fibril like structures are degraded over time leaving the rest of the surface nearly untouched (blue squares).

A clear degradation of crystalline fibrils is observable in the phase image. Moreover, we detect an increase of amorphous regions, which is in good agreement with the basic idea what CBH I is believed to do (Figure 7) [15]. However a lot of crystalline parts were not attacked indicating that CBH I need assistance from other enzymes to access these areas. As observed with the other single cellulases, the activity towards the MAC substrate is very low with respect to the enzyme loading.

### 3.3.3 CBH II

CBH II is classified as exoglucanase acting preferably on crystalline substrate parts. We know from molecular dynamic simulations that CBH II might undergo structural changes in the

exo-loop regions allowing the enzyme to act as an endoglucanase. This feature should give the enzyme an advantage on a mainly amorphous substrate [16].

During our AFM-based investigation we used a crystalline inclusion body as orientation point during the degradation process. As already seen with the complete cellulase system we did not observe degradation of the inclusion body. In addition, there were also other areas showing no change in their height profile indicating that CBH II attacks only special parts of the surface (Figure 8).

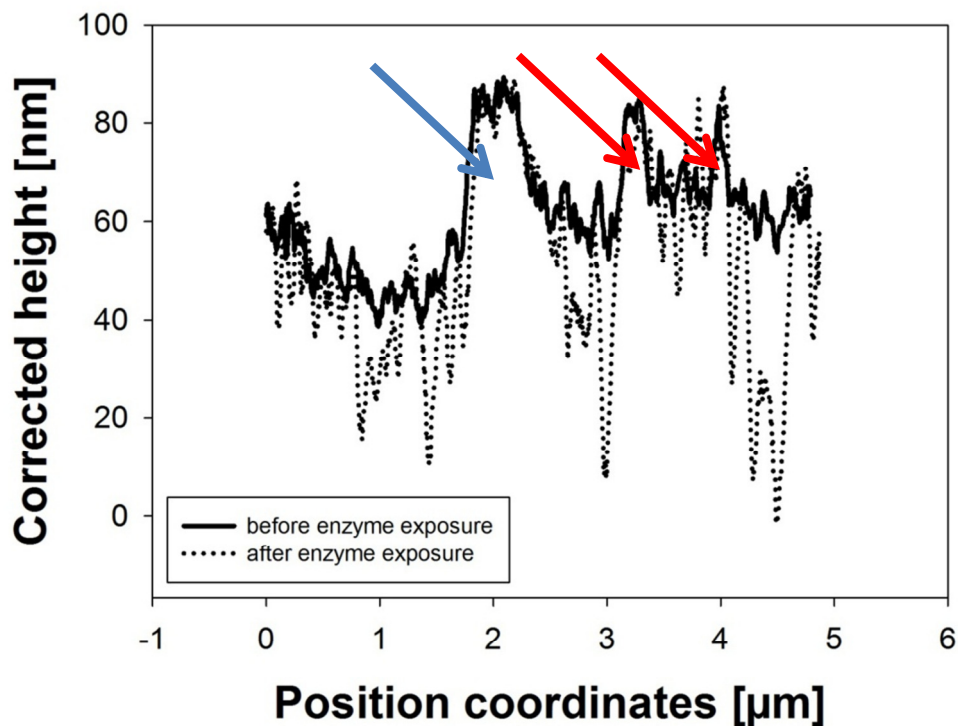


**Figure 8.** Section profile of our substrate before and after incubation with CBH II. Compared to the full cellulose system we observed a lot of untouched areas (red arrows) aside from our orientation point (blue arrow).

We also observed a clear change in the phase image towards crystalline regions indicating that there happens mainly degradation of amorphous parts. Furthermore, CBH II removes the amorphous layer from crystalline parts which is in a good agreement with the previous mentioned surface properties change. This is further supported by the appearance of fibrils on the surface as shown in Figure 9.

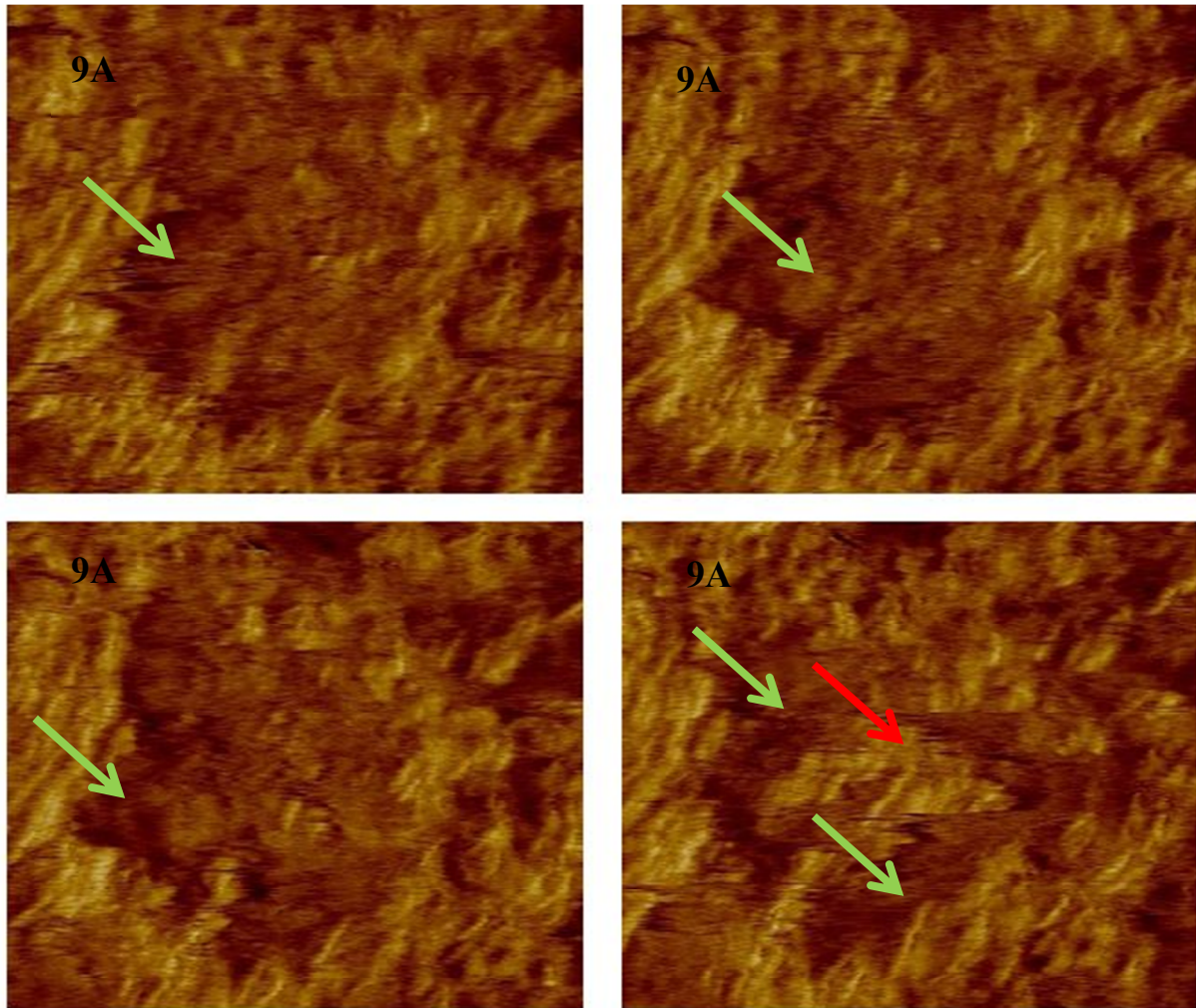


**Figure 9.** The formation of “cloud like structures” (green arrows) is clearly conceivable on amorphous parts. After those clouds move away crystalline substrate parts were revealed (red arrow). Overall, we detect an increase of crystalline areas (bright parts).

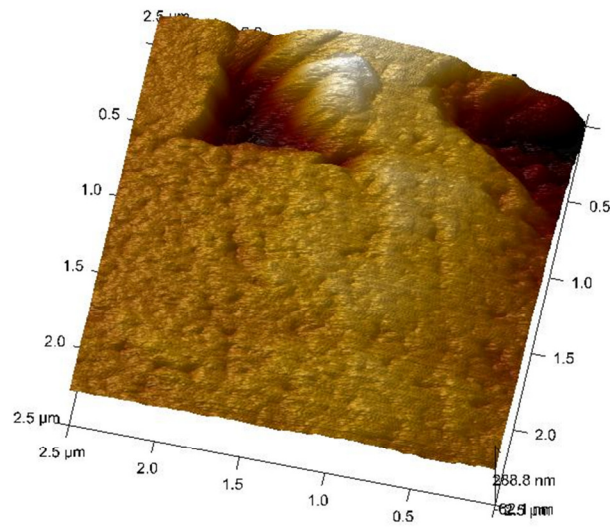
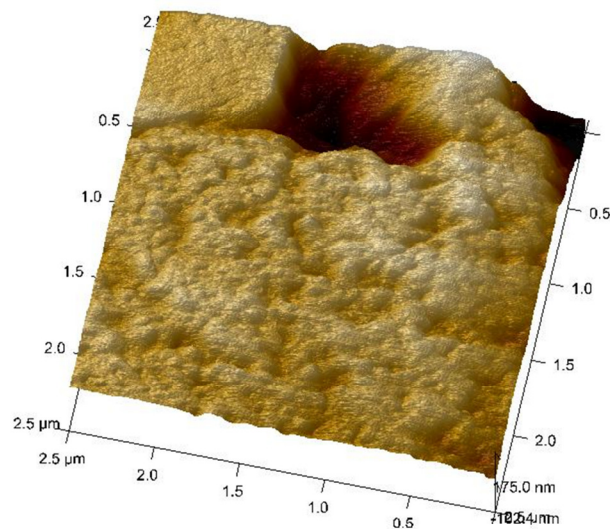
Another effect, which we only observe incubating with CBH II, was the formation of clouds on the substrate (Figure 9). Moreover, we observed movement of the clouds away from crystalline parts which were covered by amorphous material before. Based on this we conclude that these clouds refer to enzymatic activity. The clouds might arise from the high

enzyme loadings on the surface. They can be clearly distinguished in the AFM phase image due to different mechanical properties. The effect, of moving away from substrate is supported by hydrolysis data derived from our Avicel hydrolysis where a release of bound protein is observable after the point of rate retardation.

### 3.3.4 EG I

EG I is the main endoglucanase in the *Trichoderma reesei* system with a 10 % share of the whole supernatant enzyme content [14]. EG I is believed to preferably act on amorphous regions but also to introduce cuts in crystalline parts to generate new chain ends for exo-enzymes.

From our hydrolysis studies we know that EG I produce mainly glucose on our amorphous substrates. According to this, we observed a depletion of material at the border of cavities (Figure 10A and 10B). Enzymatic degradation on these border areas might result in a formation of short oligosaccharides or even glucose [17].

**10A****10B**

**Figure 10.** The MAC substrate before (A) and after (B) the incubation with EG I as a topographical image overlaid with phase information. Interestingly, we observed a widening of the cavity located in the upper centre of the picture and a degradation of the substrate at the

right site of the crystalline inclusion body. Moreover we saw a strong increase in crystalline surface area.

As indicated by the phase information there is a clear increase of higher packed material on the surface. Furthermore, we saw the degradation of small particles all over the surface leading to a mainly crystalline surface with coarser structures (Figure 10). This is a main difference between CBH II and EG I on the MAC substrate: EG I predominantly works on the surface, CBH II seems to work preferably in cavities, thereby increasing their size.

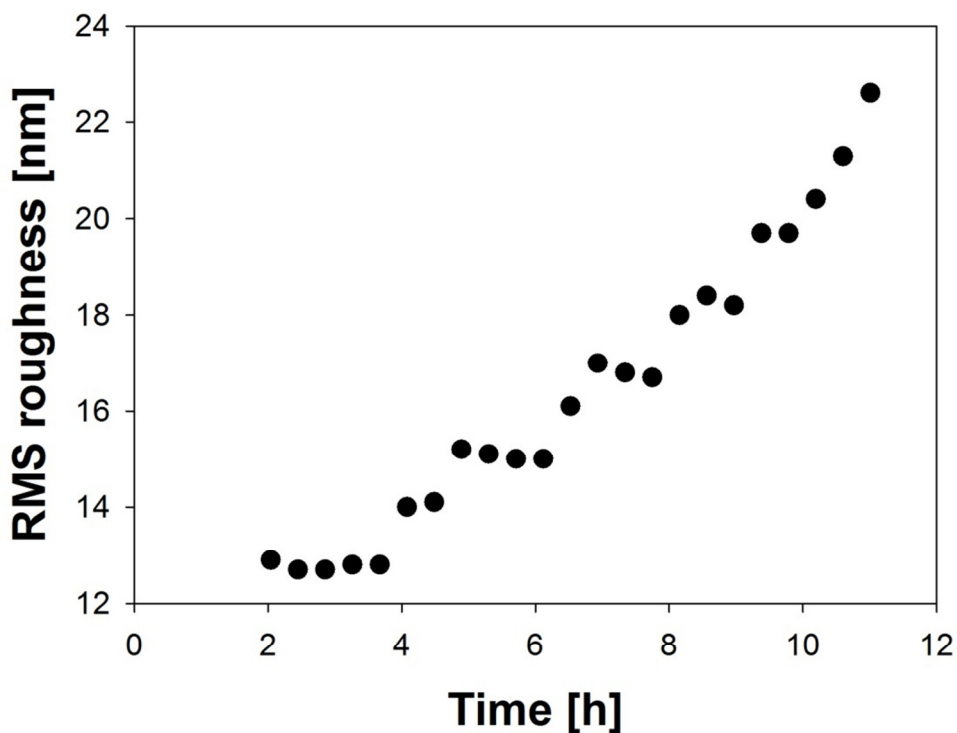


**Figure 11.** The average roughness calculated over a statistical relevant part of the surface area excluding the cavity in the upper centre. Interestingly, we observed a step-like function of the roughness increasing.

Another interesting point is that the average roughness on the surface (Figure 11) increases very slowly but in a step like function. The slow increase in the beginning is in a good agreement with our hydrolysis studies where we observed a lag phase over the first 0.7 hours incubating with 50 °C. We assume that at the beginning EG I is cutting randomly distributed over the surface which does not lead to the production of soluble sugars [18] or a noticeable change on the surface.

## 4 Appendix B – Purification of CBH I

### 4.1 Introduction

Extracellular Enzymes produced by different *Trichoderma sp.* were subject of many studies over the last decades in terms of plant valorisation via enzymatic hydrolysis. Most of those studies were performed using the model organism *Trichoderma reesei* which can be considered as the most potential producer of cellulose degrading enzymes [19].

Different approaches of enzyme purification have been probed towards *Trichoderma sp.* cellulases using mainly anion-exchange columns. Already in the early 1980s simple protocols to separate CBH I and  $\beta$ -glucosidase from the remaining fungal supernatant were established [20]. In contrast, the separation of CBH II, EG I and other endoglucanases still requires more effort like several steps of anion- and cation-exchange-chromatography [21] or the synthesis of sophisticated active groups [22] for other types of chromatography.

In our work we isolated the CBH I from *Trichoderma reesei* using “Fast Protein Liquid Chromatography” (FPLC) on an anion-exchange column for further AFM studies. Additionally we established a modified method for activity measurements using a fluorescent substrate. We performed our measurements using 4-methylumbelliferyl- $\beta$ ,D-cellobioside [23] at a lower pH as reported in literature to avoid a loss of activity and to avoid a loss of enzyme since we were working with low concentrations and low available volume.

### 4.2 Material and Methods

#### 4.2.1 Materials

All chemicals and protein standards were purchased from Carl Roth, Vienna, Austria unless otherwise stated.

#### 4.2.2 Enzyme preparation

The complete cellulase system from *Trichoderma reesei* SVG17 was produced as described by Esterbauer *et al.* [8] and supplemented with 0.05 % sodium azide for storage at 4 °C. Protein concentration was determined to be 0.62 g/l using a “Bovine Serum Albumin” (BSA) calibrated Bradford Assay [9]. Activity was determined, as recommended by IUPAC, using the well established “filter paper units” (FPU) assay [8]. According to this assay, our cellulase system had 1.3 FPU/ml.

Before use the supernatant were subjected to buffer exchange using a NAP-25 column purchased from GE Healthcare, Vienna, Austria. Buffer exchange was performed according to the manufactures protocol.

#### 4.2.3 Purification of CBH I

We performed protein separation using a Mono Q 5/50 GL Column from GE Healthcare Life Sciences and a Biorad Biologic Duo/Flow system. A Bio-Rad Model 2128 Fraction collector was used to collect 2 ml samples. The total amount of enzyme loaded was about 0.7 mg in every approach. The protocol (Table 1) for FPLC was adapted from the earlier work of Ellouz *et al* [19].

**Table 1.** FPLC Protocol (Buffer A: 20 mM TRIS-HCl; Buffer B 20 mM TRIS-HCl with 0.5 M sodium chloride)

Volume [ml]	Description	Parameters		
0.00	Collection Fractions of size 2 ml during entire run			Volume Flow
0.00	UV Detector	Turn On		
0.00	Zero Baseline (UV Detector)			
0.00	Isocratic flow	Buffer A*	100%	2.00 ml
		Buffer B**	0%	1.00 ml/min
2.00	Load/Inject Sample	Sample		6.00 ml
		Static Loop	Auto Inject Valve	0.50 ml/min
8.00	Linear Gradient	Buffer A	100% → 60%	22.0 ml
		Buffer B	0% → 40 %	1.00 ml/min
30.00	Linear Gradient	Buffer A	60% → 100%	16.0 ml
		Buffer B	40% → 100 %	1.00 ml/min
46.00	Isocratic flow	Buffer A	0%	8.00 ml
		Buffer B	100%	1.00 ml/min
54.00	End			

#### 4.2.4 Protein concentration

Concentration of the supernatant was determined using a BSA calibrated Bradford assay adapted to a 96-well-plate. 50 µl of sample was added to 200 µl Bradford Reagent and incubated for 15 minutes at room temperature. Afterward the protein concentration was measured using a wavelength of 595 nm.

#### 4.2.5 Enzymatic activity assays

For activity measurements we used the fluorescence substrate 4-methylumbelliferyl-β,D-cellobioside, which is known to be a suitable substrate for CBH I [23]. Reactions were performed continuously in a 50 µL of 50 mM sodium-acetate buffer using a substrate

concentration of 100  $\mu\text{M}$  at 40  $^{\circ}\text{C}$ . The calibration was done by using 4-methylumbelliferone as standard.

Measurements were performed with an excitation wavelength ( $\lambda_{\text{ex}}$ ) of 360 nm and an emission wavelength ( $\lambda_{\text{em}}$ ) of 450 nm using a Fluostar Omega platereader (BMG Labtech, Ortenberg, Germany).

### 4.3 Results

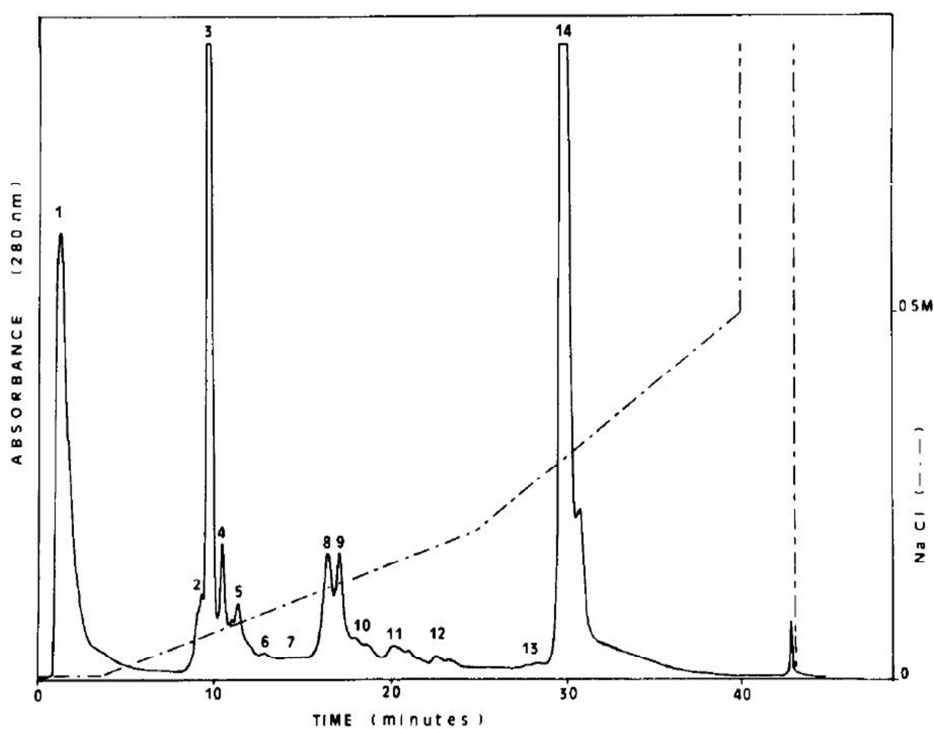


**Figure 1.** FPLC diagram as published by Ellouz et al. CBH I was eluted after 30 minutes (Peak 14). CBH II and EG I were eluted after ten minutes (Peak 3) but could not be further separated at this time.

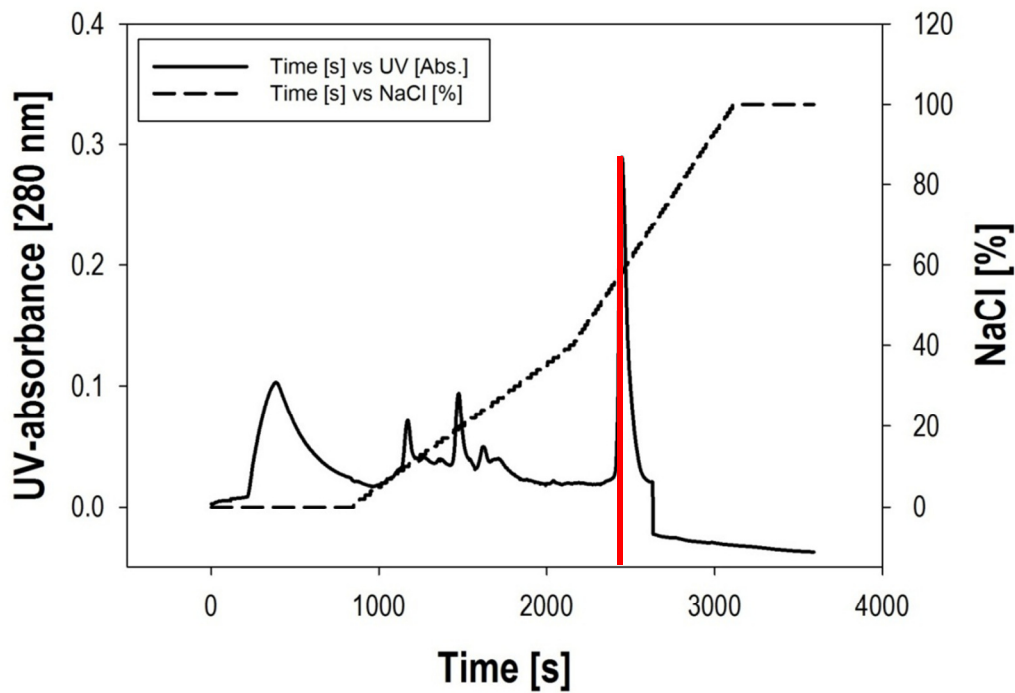


**Figure 2.** FPLC performed to isolate CBH I using a flow rate of 1.00 ml/min. CBH I elution peak is indicated by the red line and elution time is comparable to data achieved by *Ellouz et al.*

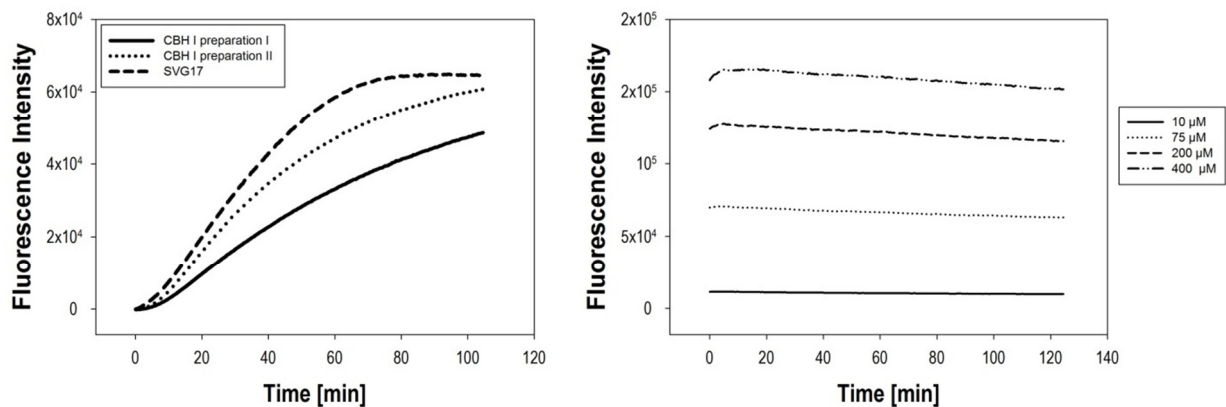


**Figure 3.** Activity measurements of different CBH I preparations in comparison to the whole supernatant was performed to examine the influence of buffer exchange immediately after

elution (left graph). Moreover we observe a decrease of the fluorescence intensity over time increasing with the concentration of the substrate (right graph). The fluorescence intensity was amplified using an internal fluorescence gain of 1200 for both experiments.

#### 4.4 Results and Discussion

As we could show the use of a Mono Q 5/50 GL provide the possibility to isolate CBH I out of buffer exchanged supernatant in a reproducible way and as described in literature (compare Figure 1 and 2).

The amount of isolated CBH I was about 80 % of the theoretical content based on the assumption that the total amount of CBH I is approximately 60 % of the entire cellulase content of the supernatant (Table 3). However, there are difficulties to compare protein concentration values of a protein mixture to single enzyme preparations. This problem arises from the fact that the Bradford Assay is based on the content of cationic and aromatic amino acids [9]. The content of these amino acids in the calibration protein BSA is up to three fold higher than in the isolated CBH I or other cellulolytic enzymes produced by *Trichoderma reesei*. This influences the measurement to show lower concentrations for CBH I as present in isolated samples.

Two different types of enzyme preparations were measured: CBH I preparation I was collected as eluted. In contrast, CBH I preparation II was immediately diluted with 50 mM sodium citrate buffer in a ratio of 1:2. This was done to avoid possible enzyme inactivation since the upper pH tolerance for cellobiohydrolases is known to be about pH 8.00 and also to dilute the sodium chloride buffer compound. As shown in Table 2, we observed different activities for the CBH I preparations indicating that the dilution step alleviate the loss of specific activity.

Regardless there might be a loss of activity because only 60 % of the supernatant protein content can be considered as CBH I. Another problem is to estimate the influence of the  $\beta$ -glucosidase, which is active towards the soluble 4-methylumbelliferyl- $\beta$ ,D-glycoside derivate [24] as proved in another experiment. As a result the exact activity of CBH I in the crude cellulose system could not be calculated.

**Table 2.** Enzymatic activities of different CBH I preparations measured using 4-methylumbelliferyl- $\beta$ ,D-cellobioside as substrate.

Enzyme preparation	$E_{Aspez}$ [ $\mu\text{mol min}^{-1} \text{mg}^{-1}$ ]
CBH I preparation I	0.14
CBH I preparation II	0.17
SVG17	0.19

**Table 3.** Enzymatic properties of the isolated CBH I compared to the crude supernatant.

	crude supernatant	purified CBH I
$C_{\text{protein}}$ [g/l]	0.35	0.17
$C_{\text{protein}}$ [g/l] corrected*	0.21	0.17
$E_A$ [ $\mu\text{mol min}^{-1} \text{ml}^{-1}$ ]	0.065	0.029
$E_{Aspez}$ [ $\mu\text{mol min}^{-1} \text{mg}^{-1}$ ]	0.19	0.17
$E_{Aspez}$ [ $\mu\text{mol min}^{-1} \text{mg}^{-1}$ ] corrected*	0.31	0.17

\*: Values are corrected due to the fact that only 60% of the overall protein content of the crude extract can be considered as CBH I.

## 4.5 Conclusions

As shown in Table 3 we are able to recover up to 48 % of the inserted protein which means that we are able to isolate about 80 % of the applied CBH I content. The corrected specific activity showed a loss of activity in the range of approximately 40 %. Unsuccessfully we were not able to determine the influence activity of  $\beta$ -glucosidase activity. This leads to the possibly that the activity of the retained CBH I is higher as calculated.

## 5 References

- [1] Quirk A., Lipkowskoki J., Vandenende C., Cokcburn D., Clark A., Dutcher J. and Roscoe S. (2010) Direct visualization of the enzymatic digestion of a single fiber of native cellulose in an aqueous environment by atomic force microscopy. *Journal of Surfaces and Colloids* **26**, 5007-13
- [2] Allison D. P., Mortensen N. P., Sullivan C. J. and Doktycz M. J. (2010) Atomic force microscopy of biological samples. *Nanomedicine and Nanobiotechnology* **2**, 618-34
- [3] Bubner P., Dohr J., Plank H., Mayrhofer C. and Nidetzky B. (2011) Cellulases dig deep: in situ observation of the mesoscopic structural dynamics of enzymatic cellulose degradation. *Journal of Biological Chemistry*, accepted November the 29<sup>th</sup>, 2011
- [4] Liu Y.-S., Baker J. O., Zeng Y., Himmel M. E., Haas T. and Ding S.-Y. (2011) Cellobiohydrolase hydrolyzes crystalline cellulose on hydrophobic faces. *Journal of Biological Chemistry* **286**, 11195-201
- [5] Igarashi K., Koivula A., Wada M., Kimura S., Penttilä M. and Samejima M. (2009) High speed atomic force microscopy visualizes processive movement of *Trichoderma reesei* cellobiohydrolase I on crystalline cellulose. *Journal of Biological Chemistry* **284**, 36186-90
- [6] Igarashi K., Uchihashi T., Koivula A., Wada M., Kimura S., Okamoto T., Penttilä M., Ando T. and Samejima M. (2011) Traffic jams reduce hydrolytic efficiency of cellulase on cellulose surface. *Science* **333**, 1279-1282
- [7] Goyal A., Ghosh B. and Eveleigh D. (1991) Characteristics of fungal cellulases. *Bioresource Technology* **36**, 37-50
- [8] Esterbauer H., Steiner W., Labudova I., Hermann A. and Hayn M. (1991) Production of *Trichoderma* cellulase in laboratory and pilot scale. *Bioresource Technology* **36**, 51-65
- [9] Compton S. and Jones C. (1985) Mechanism of dye response and interference in the Bradford protein assay. *Analytical Biochemistry* **151**, 369-374
- [10] Prasad K., Kaneko Y. and Kadokawa J. (2009) Novel gelling systems of kappa-, iota- and lambda-carrageenans and their composite gels with cellulose using ionic liquid. *Macromolecular Bioscience* **9**, 376-82

- [11] Liu H., Fu S., Zhu J. Y., Li H. and Zhan H. (2009) Visualization of enzymatic hydrolysis of cellulose using AFM phase imaging. *Enzyme and Microbial Technology*, **45**, 274-281
- [12] Zhao X., Rignall T. R., McCabe C., Adney W. S. and Himmel M. E. (2008) Molecular simulation evidence for processive motion of *Trichoderma reesei* Cel7A during cellulose depolymerisation. *Chemical Physics Letters* **460**, pp. 284-288
- [13] Eriksson T., Karlsson J. and Tjerneld F. (2002) A model explaining declining rate in hydrolysis of lignocellulose substrates with Cellobiohydrolase I ( Cel7A ) and Endoglucanase I ( Cel7B ) of *Trichoderma reesei*. *Applied Biochemistry and Biotechnology* **101**, 41-60
- [14] Lynd L. R., Weimer P. J., Van Zyl W. H. and Pretorius I. S. (2002) Microbial cellulose utilization: fundamentals and biotechnology. *Microbiology and Molecular Biology Reviews* **66**, 506–577
- [15] Våljamäe P. (2002) The Kinetics of Cellulose Enzymatic Hydrolysis. *Acta Universitatis Upsaliensis*
- [16] Zou J., Kleywegt G., Stahlberg J., Driguez H., Nerinckx W., Claessens M., Koivula A., Teeri T. and Jones A. (1999) Crystallographic evidence for substrate ring distortion and protein conformational changes during catalysis in cellobiohydrolase Cel16A from *Trichoderma reesei*. *Structure* **7**, 1035-45
- [17] Karlsson J., Siika-aho M., Tenkanen M. and Tjerneld F. (2002) Enzymatic properties of the low molecular mass endoglucanases Cel12A (EG III) and Cel45A (EG V) of *Trichoderma reesei*. *Journal of Biotechnology* **99**, 63-78
- [18] Griggs A. J., Stickel J. J. and Lischeske J. J. (2011) A mechanistic model for enzymatic saccharification of cellulose using continuous distribution kinetics I: depolymerization by EG I and CBH I. *Biotechnology and Bioengineering*, accepted September 26<sup>th</sup>, 2011
- [19] Ellouz S., Durand H. and Tiraby G. (1987) Analytical separation of *Trichoderma reesei* cellulases by ion-exchange fast protein liquid chromatography. *Journal of Chromatography A* **396**, 307-317
- [20] Tilbeurgh H. V. and Claessens M. (1984) Separation of endo- and exo-type cellulases using a new affinity chromatography method. *FEBS Letters* **169**, 215-218
- [21] Medve J., Lee D. and Tjerneld F. (1998) Ion-exchange chromatographic purification and quantitative analysis of *Trichoderma reesei* cellulases cellobiohydrolase I, II and endoglucanase II by fast protein liquid chromatography. *Journal of Chromatography A* **808**, 153–165

- [22] Ogata M., Kameshima Y., Hattori T., Michishita K., Suzuki T., Kawagashi H., Totani K., Hiratake J. and Usui T. (2010) Lactosylamidine-based affinity purification for cellulolytic enzymes EG I and CBH I from *Hypocrea jecorina* and their properties. *Carbohydrate Research* **345**, 2623-9
- [23] Marx M. C., Wood M. and Jarvis S. (2001) A microplate fluorimetric assay for the study of enzyme diversity in soils. *Soil Biology and Biochemistry* **33**, 1633–1640
- [24] Sharrock K. R. (1998) Cellulase assay methods: a review. *Journal of Biochemical and Biophysical Methods* **17**, 81-105

## 6 Supporting Information

### 6.1 Protein sequence of CBH II expressed in *Pichia pastoris*

MIVGILTTLATLATLAASVPLEERQACSSVWGQCGGQNWSGPTCCASGSTCVYSNDY  
YSQCLPGAASSSSSTRAASTTSRVSPPTTSRSSSATPPPGSTTTRVPPVGSATATYSGNPF  
VGVTPWANAYYASEVSSLAIPSLTGAMATAAAAVAKVPSFMWLDTLDKTPLMEQTL  
ADIRTANKNGGNYAGQFVVYDLPDRDCAALASNGEYSIADGGVAKYKNYIDTIRQIV  
VEYSDIRTLLVIEPDSLNLVTNLGTPKCANAQSAYLECINYAVTQLNLPNVAMYLD  
AGHAGWLGWPANQDPAAQLFANVYKNASSPRALRGLATNVANYNGWNITSPPSYT  
QGNVYNEKLYIHAIGPLLANHGWSNAFFITDQGRSGKQPTGQQQWGDWCNVIGTG  
FGIRPSANTGDSLLDSFVWVKPGGECGTSDSSAPRFDSHCALPDALQPAPQAGAWF  
QAYFVQLLTNANPSFL

## 7 Abbreviations

AFM	atomic force microscopy
BMIMCl	1-butyl-3-methylimidazolium chloride
CBD	cellulose binding domain
CI	crystallinity index
CMC	carboxymethyl cellulose
DNS	3,5-dinitrosalicylic acid
FPLC	fast protein liquid chromatography
FPU	filter paper units
MAC	mixed amorphous-crystalline
PASC	phosphoric acid swollen cellulose
RMS	root mean square
SEM	and scanning microscopy
TEM	transmission electron microscopy